University of South Carolina
Scholar Commons

Theses and Dissertations

Spring 2023

Physics-Based and Behavioral Models for Fuel Cells

Charles Chima Anyim

Follow this and additional works at: https://scholarcommons.sc.edu/etd

 Part of the Electrical and Computer Engineering Commons

Recommended Citation

Anyim, C. C.(2023). *Physics-Based and Behavioral Models for Fuel Cells.* (Master's thesis). Retrieved from https://scholarcommons.sc.edu/etd/7323

This Open Access Thesis is brought to you by Scholar Commons. It has been accepted for inclusion in Theses and Dissertations by an authorized administrator of Scholar Commons. For more information, please contact digres@mailbox.sc.edu.

PHYSICS-BASED AND BEHAVIORAL MODELS FOR FUEL CELLS

by

Charles Chima Anyim

Bachelor of Engineering
University of Benin, 2016

Submitted in Partial Fulfillment of the Requirements

For the Degree of Master of Science in

Electrical Engineering

College of Engineering and Computing

University of South Carolina

2023

Accepted by:

Enrico Santi, Director of Thesis

Krishna Mandal, Reader

Cheryl L. Addy, Interim Vice Provost and Dean of the Graduate School

© Copyright by Charles Chima Anyim, 2023

All Rights Reserved.

DEDICATION

This Thesis is dedicated to God almighty for his endless mercies and provisions for me; all knowledge and understanding concerning this Thesis comes from God. I would also thank my parents and siblings for their love and encouragement in completing this research.

ACKNOWLEDGEMENTS

First and foremost, I offer my deepest gratitude to my Advisor, Dr. Enrico Santi, for his constructive criticism and direction throughout my thesis. I would also love to extend my appreciation to other members of my research team who helped in one way or the other in the course of this research.

ABSTRACT

In recent times there has been renewed interest in fuel cells for electricity production, especially for transportation applications. Fuel cells are attractive because the electricity production process from chemical energy does not cause pollution, and no carbon emissions occur. In this work, we will focus on Proton Exchange Membrane (PEM) fuel cells that use hydrogen and oxygen to generate electricity, producing only electricity, heat and water. If hydrogen can be produced in a green, non-polluting way, fuel cells can truly be an environmentally benign energy source.

In this work, we will look at the modeling of a fuel cell system. In particular, we will consider two different types of models: we will examine a physics-based model available in MATLAB/Simulink and develop a behavioral model based on interpolation of operating characteristics available from a vendor. The advantage of this second approach is that the fuel cell system can be modeled with limited information on the system itself since all the detailed system information needed to parameterize a physics-based model is not required.

TABLE OF CONTENTS

LIST OF TABLES

LIST OF FIGURES

LIST OF SYMBOLS

W	Watts
kW	Kilowatts
kv	kilovolts
A	Amperes
v	Voltage
H	Hydrogen
O	Oxygen

LIST OF ABBREVIATIONS

CHP ..... Combined Heat and Power

CO ..... Carbon dioxide

HT-PEMFC ..... High-temperature Proton Exchange Membrane fuel cell

MATLAB ..... Matrix Laboratory

PAFC ..... Phosphoric Acid Fuel Cell

PEM ..... Proton Exchange Membrane

PEMFC ..... Proton Exchange Membrane Fuel Cells

RL ..... .resistor and inductor in series

UAV ..... Unmanned Aerial Vehicle

CHAPTER 1

INTRODUCTION

1.1 BACKGROUND

Proton Exchange Membrane Fuel Cells (PEMFCs) are one of the most promising renewable energy source systems, with zero emissions, a low operating temperature, quick startup, and a 60 percent efficiency [1,2,3]. As a result, fuel cell applications range from aerospace and automotive vehicles to small and large-scale power production facilities, portable power generators, combined heat and power (CHP), and backup power [4,5,6]. Fuel cells as a source of energy have been studied extensively over the last five decades [7,8,9,10]. Proton exchange membrane fuel cells (PEMFCs), which are ecologically benign energy conversion devices, have gotten a lot of interest in recent years as a result of rising concerns about air pollution from internal combustion engines (ICE) and depletion of fossil fuel sources [11,12].

Most of the research on this subject (PEMFC) has been conducted in various nations across the world, with China and the United States producing the most papers [13]. Review papers provide an overview of the literature regarding PEMFCs. A good example is [14] which describes membrane electrode array manufacturing alternatives, synthesis

methods, and bipolar plate manufacturing choices while reviewing the design and construction of PEMFCs.

In this research, two fuel cell models are considered, a physics-based model and a behavioral model. The first one is the power fuel cell model available in MATLAB/Simulink. This physics-based model was used for the case of a resistive and inductive load in series connected to it. The second model is a behavioral model that was developed as part of this research effort. The model utilizes data provided by a fuel cell manufacturer and uses an interpolation and extrapolation approach to determine the fuel cell characteristics as a function of operating point. This was achieved using the interp1 and scatteredInterpolant functions provided in the MATLAB/Simulink environment.

1.2 RESEARCH GOAL

The goal of this research is to examine two different fuel cell models used to represent fuel cell characteristics, including the current, voltage, efficiency, and fuel and air utilization of the fuel cell.

Objectives of the thesis include:

1.) To simulate the voltage, current, stack consumption, efficiency, fuel, and air utilization characteristics using the physics-based power fuel model in MATLAB/Simulink.

2.) To develop a behavioral model of a fuel cell that uses the scatteredInterpolant function model in MATLAB/Simulink to obtain fuel cell characteristics at a desired operating point.

3.) To describe the interp1 function model and how it can be used to generate additional data points.

The result of this study shows how we can successfully use the fuel cell for a resistive and an inductive load in series and how more data points needed for fuel cell-powered aircraft research can be generated.

1.3 THESIS STRUCTURE

This thesis is organized in five main chapters. The first chapter contains the introduction, background, research goals and objectives. The second chapter presents a literature review on PEM fuel cells. The third chapter describes the methodology used in this study. The fourth chapter presents the results and discussion of the study. The final chapter presents the conclusion and future work that can be done to improve the existing method used in this study.

CHAPTER 2

LITERATURE REVIEW

In this chapter, an overview of research work related to fuel cells is provided. This chapter will discuss the application and studies conducted on fuel cells over time.

PEM fuel cells must manage water production while reducing the costs used in computerized systems and operations in a commercial aircraft system. This is achieved by optimizing the oxygen concentrations, temperature, and mass density of the fuel cell [40]. Using the knowledge that commercial aircraft use two main courses to provide electricity throughout a flight phase which are generators and auxiliary power units (APUs), like in the case of an emergency in a flight, but in addition to that, some ground power units are used to provide power when a plane is parked. These power sources (APU and generators) are basically replaced with PEM fuel cells in this case [40]. In the case of aircraft and locomotives using a PEMFC for powering devices, it is good to consider how the operation of the fuel cell is affected by its water management for a limited range during its operation as well as the overall effect of water management in the PEMFC. This is true as water management greatly affects the fuel stack system architecture as well as its operating parameters [22]. Several studies have looked at how system analysis can be performed using relatively simple and computationally efficient proton exchange membrane fuel cell models as well as data that were obtained through various experiments via interpolation [16 – 22]. In addition, excess gases like oxygen are

controlled using a system based on PEMFC and UAV cells. Using a simple model, a PEMFC is built for this function, and there is a significant reduction in the loss of power and the amount of stress associated with the system is greatly improved [38].

For aircraft applications, fuel cells can significantly reduce the amount of emissions into the environment through underground operations of taxiing in airports by aircraft. The use of an external fuel cell ensures not only environmental protection but also provides other benefits to the aircraft, like not adding more weight to the aircraft [15]. Normally, aircraft do their taxiing using the main engines inside; this way, carbon dioxide is released into the environment, thus causing air pollution, which is a major concern as we are faced with a serious threat of global warming. In a new system proposed, all the engines that were used before would be switched off; therefore, the aircraft will not be using fuel to taxi; rather, the PEMFC will be utilized [15].

Fuel cells alongside supercapacitors make for high efficiency in systems as this saves power and also minimizes pollution in electric aircraft, motor grids, and motor vehicles [31, 32]. For aircraft that utilize PEMFCs, pressure is of significant importance. When the pressure is increased, the performance of the fuel cell also increases. This is one of the operating factors that is considered in order to effectively use fuel in aeronautical spaces [33]. Conversely, the decrease in pressure will lead to a significant decrease in the performance of the fuel cell [34-37]. This should be avoided if the fuel cell is expected to perform optimally and efficiently. Also, there are significant benefits to operating the PEMFCs stacks at lower current densities [20].

PEMFCs have been deployed in high-duty vehicles by developing a strategy that saves power through the use of an auxiliary power unit (APU), mostly in high-duty

vehicles [38]. The APU is designed to have a fuel cell and a battery that contains lead acid. This setup ensures effective control of power in the APU. APUs have been experimented with as an alternate method that can reduce the amount of fuel used hence controlling emissions to the environment [38]. Multiple fuel cell usage in vehicles and motorcycles, especially in the popular Taiwan Electrical Fuel cell Power Scooters have shown that fuel cells can be easily deployed and can be of great benefit as a source of power [41-43]. In another study, the case of a developed system that uses fuel cells instead of ignition engines in heavy-duty vehicles was analyzed. The fuel cell engine that was developed is seen to show a better use of fuel and has a high energy efficiency compared to combustion engines. A lot of space is also saved because the fuel cell engine takes up little space compared to the combustion engine. The value of the new system that has been developed in terms of efficiency is way higher than those of combustion engines. This study found that when using a fuel cell engine, the operating power system is effective in locomotives and can be used in other systems that require highly efficient power units that require little space [39].

CHAPTER 3

METHODOLOGY

The methodology is divided into two parts. The first part is the physics based model that covers the laws that govern the operation of a fuel cell. Here, the power fuel cell model, which is a model in MATLAB/Simulink that incorporates the blocks in figure 3.1 is utilized. This model is used in this reasearch to explain the operation of the fuel cell using an RL (resistor and inductor in series) load. The second part covers the behavioural modeling approach which makes use of scatteredInterpolant function and interp1 function to find additional data points. The scatteredInterpolant and Interp1 function models were used to provide additional data points needed for the fuel cell-powered aircraft in this research.

3.1 Physics Based Model

The physics based model covers the operation of an inbuilt fuel cell model in MATLAB/Simulink. The operation of the in built fuel cell called power_fuel_cell is explained below. The equations responsible for the operation of the fuel cell stack is also explained below.

3.11 Power Fuel Cell Model

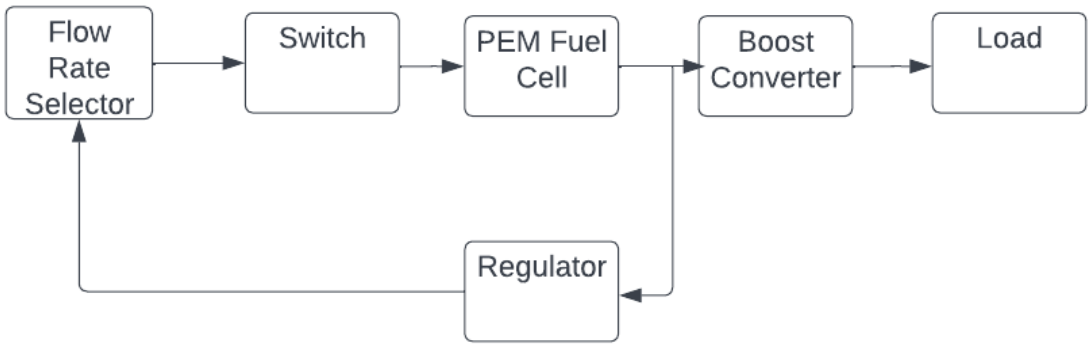

Figure 3.1 Block diagram of the power fuel cell

3.111 The Flow Rate Selector Block

The contents of the flow rate selector block are shown in figure 3.9. It contains the following blocks that determine the desired signal that is fed into the fuel stack at any given time.

3.1111 The Saturation Block

Figure 3.2 The saturation block
The saturation block provides an output that is within the limit set by the upper and lower saturation of the input signal.

3.1112 The Switch

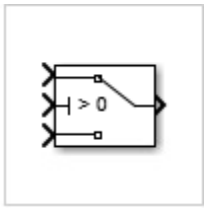

Figure 3.3 The switch block

The switch block has 3 inputs and an output. The first and third inputs are the data input, while the second input is the control input. Based on the criteria set for the control input, if the criterion is met, the output will be the data from the first input, otherwise, the output will be the data from the third input.

3.1113 The Ramp

Figure 3.4 The ramp block

The Ramp block generates the signal needed. The block contains an initial output, start time, and slope, which enables the signal generated to start at a specific time and value and to change by a specified rate based on the value of the slope entered.

3.1114 The Clock

Figure 3.5 The clock block

The Clock is used when other blocks need the simulation time in order to execute an operation. The block gives the current simulation time.

3.1115 The Compare to Constant Block

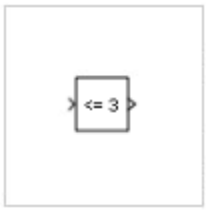

Figure 3.6 The compare to constant block

The Compare to Constant block compares an input signal to a constant. It is made up of a constant block and a relational operator block. In this operation, the relational operator used is ‘greater than’. The relational operator, and consequently the Compare to Constant block, gives an output that is ‘True’ if the first input (data coming in) is greater than the second input (The value of the constant specified in the constant block).

3.1116 The Edge Detector

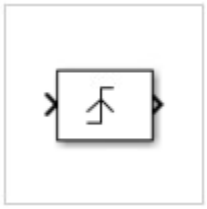

Figure 3.7 The edge detector block

The Edge detector block is designed to detect a rising edge, falling edge or both. For this particular case, the edge detector is set to detect a rising edge.

3.112 The Sample and Hold

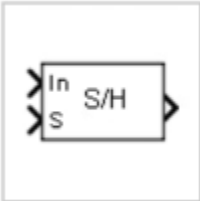

Figure 3.8 The sample and hold block

The Sample and Hold block consist of two inputs and one output. These are the In, S, and Out. The In is the input signal, the S is the control signal, which should be a Boolean (True / False,) and the Out which is the required output signal. The function of the Sample and Hold block is to transfer to the output the In (input signal) as long as S (control signal) is true. When the control signal S is false, the block holds the output.

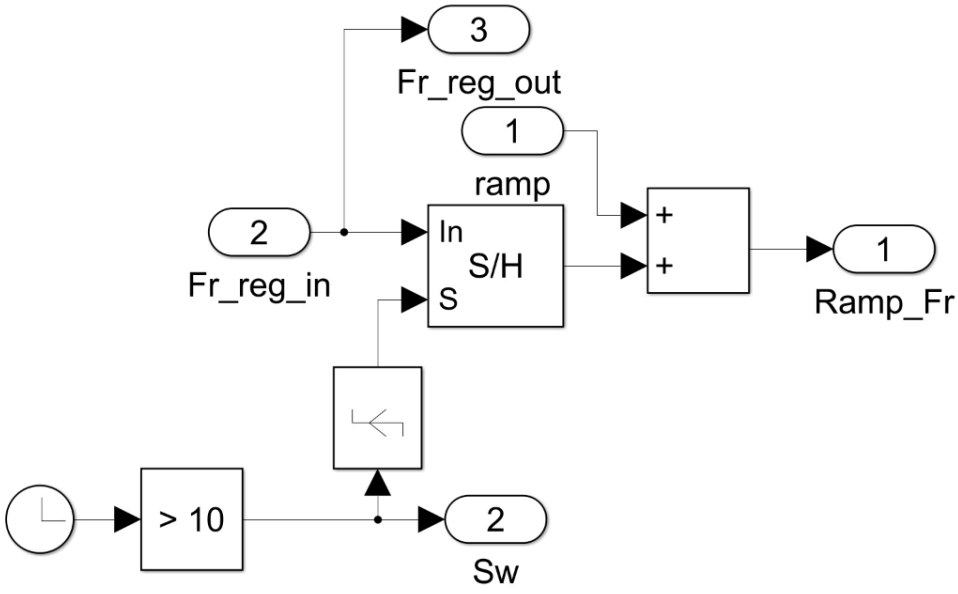

Figure 3.9 The blocks that make up the flow rate selector

In summary, the flow rate selector receives two inputs and gives out three outputs. The two inputs come from the ramp and the flow rate regulator. The three outputs are the Ramp_Fr, Sw and Fr_reg_out in figure 3.9. These three outputs go into a switch outside the flow rate selector. This switch is the final step in determining which flow rate goes into the fuel stack. The clock depicts the simulation time compared with the value of the constant in the compare to constant block. The compare-to-constant block compares the current simulation time to the constant value specified. In this case, the constant value specified is 10 seconds. Therefore, when the simulation time is above 10 s, the control of the switch is activated (the criterion is met), and the edge trigger is on a rising edge. At this point, the switch outside the flow rate regulator enables the signal coming into input 1 (Ramp_Fr), and this goes into the fuel cell stack since the criterion is met.

The signal coming from the Ramp_Fr is the sum of the signal coming from the flow rate regulator and the signal coming from the ramp. Whenever the edge trigger is at a rising edge, the criterion of the control S, of the Sample and Hold is met, and the input signal coming from the flow rate regulator drives to the output, where it is added with the input from the ramp and is fed to the fuel cell stack. The flow rate regulator block calculates the required hydrogen flow rate to have a nominal hydrogen utilization of 99.56%. The flow rate selector block selects one of two possible hydrogen flow rates. The first is at time $t < 10s$, the flow rate calculated by the flow rate regulator block, and the second is at time $t > 10s$, when the flow rate is obtained by adding to the flow rate at time 10s sampled by the Sample & Hold block and a ramp that increases the flow rate up to 85lpm (liter per minute) limited by the saturation block.

Therefore, for the first 10s, the hydrogen utilization rate is the nominal 99.56%, but it goes down after $t = 10s$ due to the increase in the fuel flow rate.

3.112 The PEM Fuel Cell Stack

In the case of fuel cells, the 'Gibbs free energy' is the energy available to do external work. This is obtained by neglecting any work done by changes in pressure and/or volume, where the 'external work' involves moving electrons around an external circuit or, better still, any work done by a change in volume between the input and output is not harnessed by the fuel cell. The energy released in a fuel cell can be deduced from the Gibbs free energy of formation ΔGf. This change (Gibbs free energy of formation) is the difference between the Gibbs free energy of the outputs or products and the Gibbs free energy of the inputs or reactants.

$$\Delta Gf = Gf \text{ of products} - Gf \text{ of reactants} \quad (3.1)$$

The quantities in equation (3.1) are represented in moles. Moles are a measure of how many elementary quantities of a given substance are in an object or sample. A mole is defined as containing exactly 6.022 x 10^{23} (Avogadro's number) elementary entities. Therefore, a mole of electrons can be seen as 6.022 x 10^{23} electrons. If we represent this by *N*, the *Faraday constant F* can be calculated.

$$F = N \cdot e = 96485 \text{ C} \quad (3.2)$$

where e is the charge of the electron, and the value is 1.602 x 10^{-19} C

The electromotive force of the PEM FC can be calculated from the basic reaction of a PEM fuel cell:

$$2H_2 + O_2 \rightarrow 2H_2O \quad (3.3)$$

The two partial reactions at the anode and cathode are

$$2H_2 \rightarrow 4H^+ + 4e^- \quad (3.4)$$

$O_2 + 4e^- + 4H^+ \rightarrow 2H_2O$ (3.5)

From the equations above, it can be seen that 2 electrons pass around the external circuit for each molecule of water produced. Hence for every mole of hydrogen used, 2N electrons pass around the external circuit, where N is Avogadro's number. Connecting this to the Faraday constant in equation (3.2)

$-2F = -2\ N\ e$ coulombs (3.6)

Given that the electrical work done responsible for moving a charge around a circuit is

Electrical work done = charge × voltage = $-2FE$ joules (3.7)

Therefore, the Gibbs free energy (considered in the mole form) released in a theoretical system assuming there are no losses can be expressed as

$\Delta g_f = -2F \cdot E$ (3.8)

The electromotive force (EMF) in a PEM FC can be expressed as

$\Delta E = \frac{-\Delta g_f}{2F}$ (3.9)

3.113 Summary of some useful equations

In a chemical reaction of the type of fuel cell, where z electrons are transferred for every molecule of fuel, the electromotive force is given by

$\Delta E = \frac{-\Delta g_f}{2F}$ (3.10)

$Efficiency = u_f \frac{V}{1.48}\ x\ 100\%$ (3.11)

where u_f is the fuel utilization and V the is the voltage per cell.

Gibbs free energy also changes based on the reactant and product pressure and concentration. The relationship between the activity of the reactant and product in an electrochemical reaction is given by

activity $a = \frac{P}{P^0}$ (3.12)

where P is the partial pressure of the gases and P^0 is the standard pressure.

Therefore, the Gibbs free energy can be written as

$$\Delta g_f = \Delta {g_f}^0 - RT \ln\left(\frac{a_{H_2}.a^{\frac{1}{2}}{}_{O_2}}{a_{H_2O}}\right) \quad (3.13)$$

Substituting the equation above into equation

$$E = \frac{-\Delta {g_f}^0}{2F} + \frac{RT}{2F}\ln\left(\frac{a_{H_2}.a^{\frac{1}{2}}{}_{O_2}}{a_{H_2O}}\right) \quad (3.14)$$

$$E = E^0 + \frac{RT}{2F}\ln\left(\frac{a_{H_2}.a^{\frac{1}{2}}{}_{O_2}}{a_{H_2O}}\right) \quad (3.15)$$

Given that $a_{H_2} = \frac{P_{H_2}}{P^0}$, $a_{O_2} = \frac{P_{O_2}}{P^0}$, $a_{H_2O} = \frac{P_{H_2O}}{P^0}$

$$E = E^0 + \frac{\mathrm{RT}}{2F}\ln\left(\frac{P_{H_2}.P^{\frac{1}{2}}{}_{O_2}}{P_{H_2O}}\right) \quad (3.16)$$

Where E^0 is the cell EMF at standard pressure.

Equation (3.16) is the Nernst equation.

In addition, a fuel cell is preferably operated at a high voltage because at a high voltage, the difference between the actual operating voltage and the reversible no loss voltage is significantly less when the cell is operating at a higher temperature. So even though the no loss voltage is lower at higher temperatures, the operating voltage is higher because of a smaller voltage drop at higher temperatures.

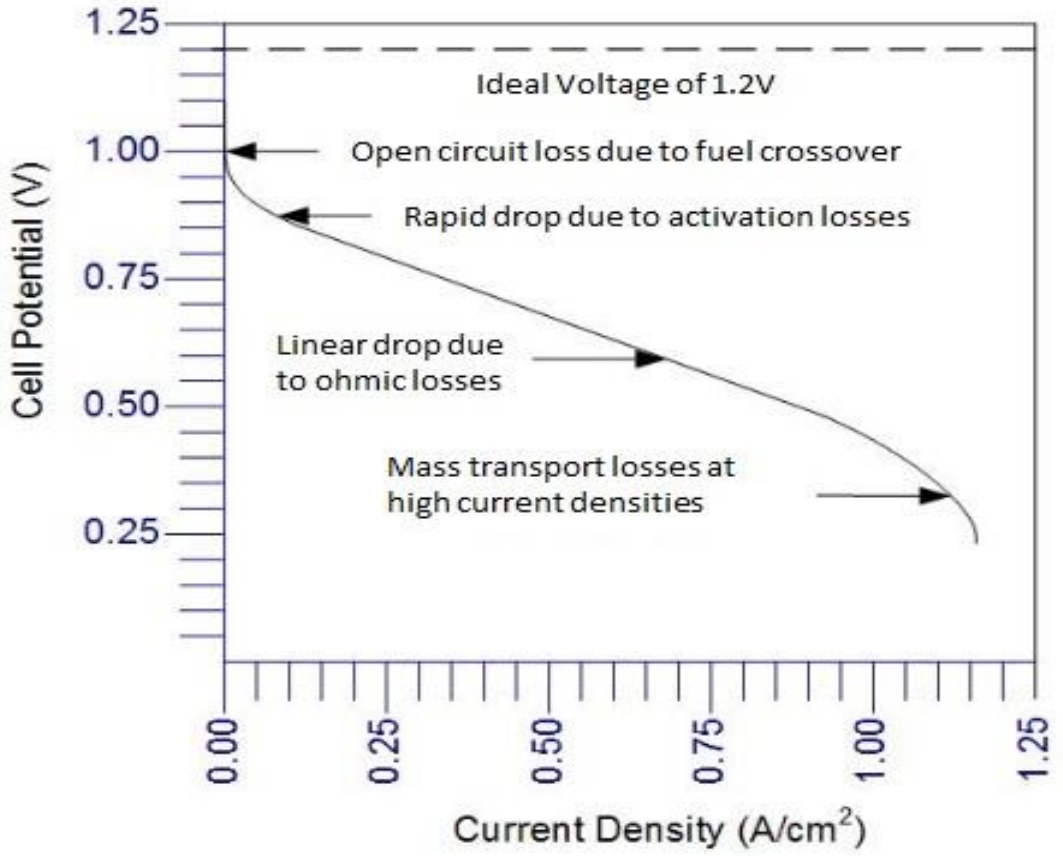

Figure 3.10 PEMFC Polarization curve

The polarization curve shown above gives a pictorial view of the losses in fuel cells. The losses are explained below.

3.114 Activation Losses

These losses, which are responsible for the non-linear voltage drop at low current densities and are caused as a result of slowness of the reaction that takes place at the surface of the electrodes, thereby leading to a drop in the voltage generated. The overvoltage at the surface of the electrode is given by

$$\Delta V_{\text{act}} = A \ln\left(\frac{i}{i_0}\right) \qquad (3.17)$$

where the constant A is higher for a slow electrochemical reaction and the current density i_0 which is the current density at the point where the overvoltage begins to move from zero is higher if the electrochemical reaction is faster.

Equation (3.17) is referred to as the Tafel equation.

The constant A is given by

$$A = \frac{\mathrm{RT}}{2\alpha F} \tag{3.18}$$

where α is the charge transfer coefficient which depends on the material the electrode is made from and usually fall between the range 0 to 1.0.

Hence for a fuel cell with no other losses aside the activation losses, the voltage will be given by

$$V = E - A \ln\left(\frac{i}{i_0}\right) \tag{3.19}$$

3.115 Fuel Crossover and Internal Currents

Fuel crossover occurs when some fuel diffuses from the anode to the cathode through the electrolyte thereby reacting with the oxygen and producing no current from the cell. This results in wastage of fuel. In other words, the crossing over of one molecule of hydrogen from the anode to the cathode leads to the wastage of two electrons.

Calculating the fuel cell crossover is made possible by considering i_n which is the internal current density. The voltage as a result of the overvoltage and the fuel crossover is given by

$$V = E - A \ln\left(\frac{i + i_n}{i_0}\right) \tag{3.20}$$

3.116 Ohmic Losses

These losses are due to electrical resistance in the electrodes and the movement of ions in the electrolyte. The voltage drop is given by

$$V = IR \tag{3.21}$$

Since this occurs over a given area, it is preferable to consider the voltage drop over 1 cm^2 of the fuel cell. This is considered as the 'area-specific resistance' and is given by

$$\Delta V_{\text{ohm}} = ir \tag{3.22}$$

where i is the current density in mA cm^{-2} and the area specific resistance is in kΩ cm^2

3.117 Mass transport or Concentration Losses

A change in the concentration of the gases at the anode and cathode can lead to reduction in partial pressure and subsequently a reduction in the voltage of the fuel cell. As oxygen supplied in the form of air reaches the cathode, there will be a drop in the concentration of oxygen in the region close to the location where the oxygen is extracted. The drop in concentration is further enhanced by the current taken from the fuel cell and the rate at which the oxygen is replaced and the air circulation around the cathode. This leads to a reduction in the partial pressure of the oxygen. In a similar manner, the hydrogen at the anode also experiences a drop mainly due to resistance of the flow of hydrogen through the supply duct, electrical current drawn from the cell and other physical characteristics. This drop can be calculated as follows.

The voltage drop due to pressure changes in hydrogen is given as

$$\Delta V = \frac{\mathrm{RT}}{2F} \ln\left(\frac{P_2}{P_1}\right) \tag{3.23}$$

This equation can be transformed by postulating a limiting current density i_1 which occurs at a point when the fuel is used up at a rate equal to the maximum possible supply speed of the gases.

In addition, the corresponding pressure at this point which is just about to reach zero is given as P_1. Therefore, the pressure P_2 at any given current density i can be represented by

$$P_2 = P_1\left(1 - \frac{i}{i_1}\right) \tag{3.24}$$

Introducing the above equation into equation (3.23) gives

$$\Delta V = -\frac{\mathrm{RT}}{2F}\ln\left(1 - \frac{i}{i_1}\right) \tag{3.25}$$

This is the voltage drop due to mass transport losses and the negative sign represents a drop in voltage. Another formula which gives a better result but without any theoretical basis but entirely empirical that was introduced due to inaccuracies in results of the above formula as a result of challenges faced in fuel cell supplied with air rather than pure oxygen, lower temperature fuel cell and hydrogen mixed with other gases is

$$\Delta V_{\mathrm{trans}} = m\exp(ni) \tag{3.26}$$

where m is approximately 3 x 10^{-5} V and n is approximately 8 x 10^{-3} cm^2 mA^{-1}

3.118 Combining the losses.

If we consider the losses encountered in the PEM fuel cell, the voltage of the fuel cell at any point by taking into consideration the losses are given by

$$V = E - \Delta V_{\mathrm{ohm}} - \Delta V_{\mathrm{act}} - \Delta V_{\mathrm{trans}} \tag{3.27}$$

$$V = E - ir - A\ln\left(\frac{i + i_{\mathrm{n}}}{i_0}\right) - m\exp(ni) \tag{3.28}$$

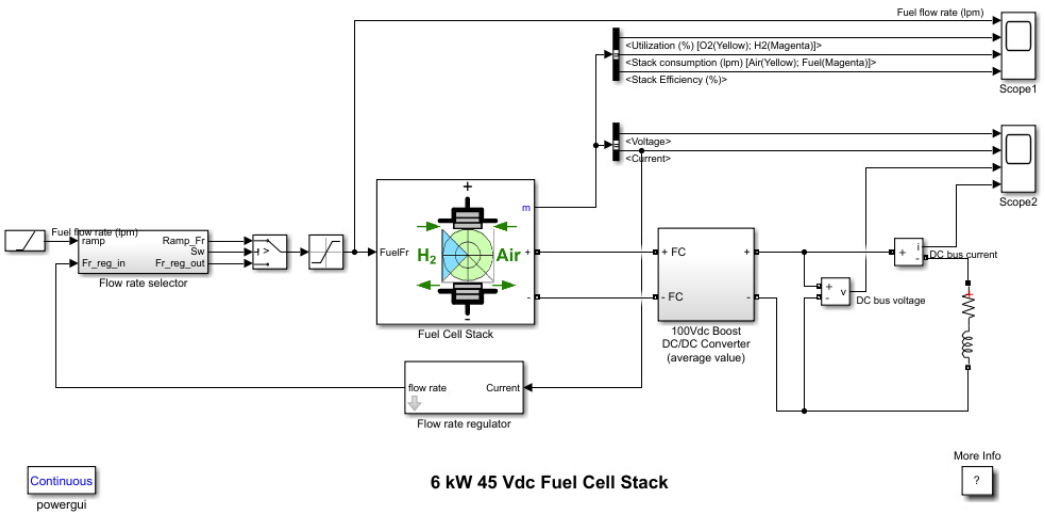

Figure 3.11 Simulink view of the Power Fuel cell

3.119 The Regulator block

$$V_f = \frac{60000 * R *(273 + T) * N * I_{fc}}{2 * F * \left(101325 * P_f\right) * \frac{U_{fH2}}{100} *(\frac{H_2\ composition}{100})} \quad (3.29)$$

R = 8.3145 J/(molK)

T = Operating Temperature (c) = 65 degree Celsius

F = 96485 A s/mol.

P_f = Fuel pressure = 1.5 bars

U_{fH2} = Nominal Hydrogen utilization = 99.56 %

H_2 = Hydrogen Composition = 99.95 %

N = Number of cells = 65

3.120 Boost Converter

A boost converter is a DC-to-DC power converter that produces a dc output voltage that is greater in magnitude than the dc input voltage. The circuit diagram in figure 3.12 shows a simple boost converter circuit diagram. Although, the power fuel cell model uses an IGBT switch rather than a MOSFET, the principle of operation is similar. The equation for the functionality of the boost converter can be gotten by applying small ripple approximation, the principles of inductor volt-second balance and capacitor charge balance in order to determine the output voltage and inductor current of the boost converter.

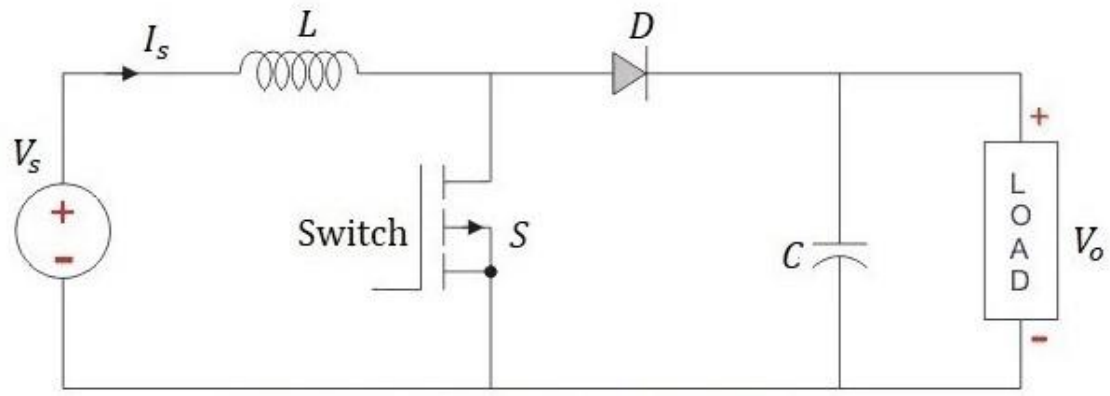

Figure 3.12 The boost converter circuit diagram

During the switch on-time, the equations describing system operation are given by

$$v_{\mathrm{L}} = V_{\mathrm{s}} \tag{3.30}$$

$$i_{\mathrm{C}} = -\frac{V}{R}(1 - e^{-Rt/L}) \tag{3.31}$$

During the switch off-time, the equations describing the system are given by

$$v_{\mathrm{L}} = V_{\mathrm{s}} - V_{\mathrm{o}} \tag{3.32}$$

$$i_{\mathrm{C}} = I - \frac{V}{R}(1 - e^{-Rt/L}) \tag{3.33}$$

Where:

v_{L} is the voltage in the inductor in the first half.

V_{s} is the input voltage volts

i_{C} is the capacitor current

t is the time in seconds

L is the inductance in Henries.

The load is an RL circuit with Time Constant that is equal to L/R. V/R represents the final steady state current value after five-time constant values.

The voltage conversion ratio $M(D)$ which is the ratio of the output voltage to the input voltage is given as

$$M(D) = \frac{V_{\mathrm{o}}}{V_{\mathrm{s}}} = \frac{1}{1-\mathrm{D}} \qquad (3.34)$$

It is the desire that all the essential parameters fall within a defined range hence we cannot just set the dc-dc converter duty cycle to a single value and expect a constant output at every point in time, hence this creates the need for a feedback system. The negative feedback helps to adjust the duty cycle of the switching element automatically in order to obtain the desired output voltage.

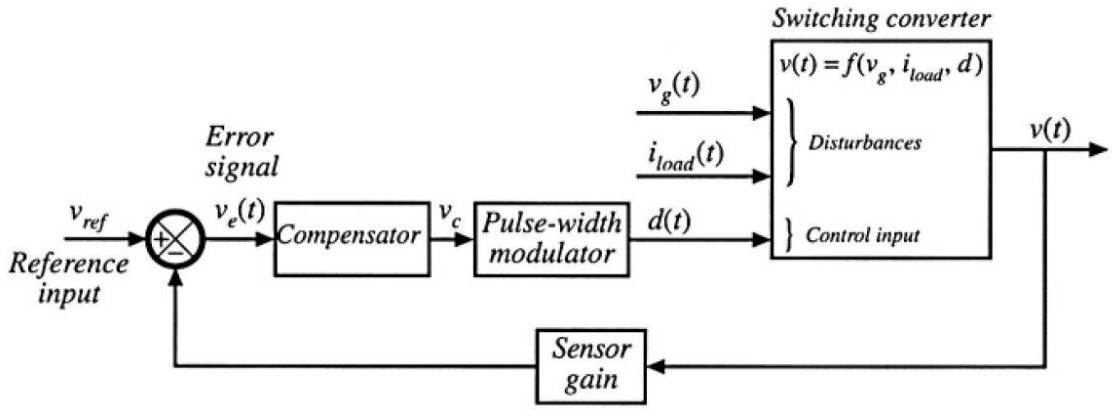

Figure 3.13 The feedback system for the switching element.

The feedback system is shown in figure 3.13. The output voltage from the converter is measured with a sensor, in this case the voltage measurement sensor. The output of the voltage measurement sensor is then multiplied by a gain of H(s)v(s) which is compared to the reference input voltage. Feedback action makes H(s)v(s) equal to V_{ref} rejecting the disturbances. Next is the error signal which is the difference between the V_{ref} and the H(s)V(s). In an ideal boost converter setup, the error signal is zero but in practice, the error signal is nonzero, but it is significantly small. The compensator helps in obtaining a small error. The output voltage at this point is a multiple of the compensator gain. A large compensator gain leads to a small error and enables the output to follow the reference input with good accuracy before it is fed to the pulse width modulator which provides the appropriate duty cycle.

3.2 Behavioral Modeling Approach

The behavioral modeling of the fuel cell stack makes use of few data points and uses interpolation to determine the relationship between the various data points and to also create more data points. Interpolation is a technique for adding new data points within a range of a set of known data points.

The two types of interpolation employed in this research are scattered data interpolation and linear interpolation.

3.21 scatteredInterpolant Function Model

The scattered data interpolation is a method used to find the value of a given data based on some defined data points that do not have any structure or order between their relative locations. This means that the data points are not necessarily even spaced or on a regular grid. There are several techniques that can be used for scattered data interpolation. The choice of method will definitely depend on the specific characteristics of the data and the desired level of accuracy. Some methods that can be used include the radial basis function interpolation, kriging, and Delaunay triangulation. The MATLAB scatteredInterpolant function which was used in this research makes use of Delaunay triangulation which is a triangulation that is equivalent to the nerve of the cells in a Voronoi diagram, i.e., the triangulation of a convex hull of the points in diagram in which every circumcircle of a triangle is an empty circle. A picture of how the triangulation is constructed for a set of data in a 2D plane is shown in figure 3.14 and 3.15.

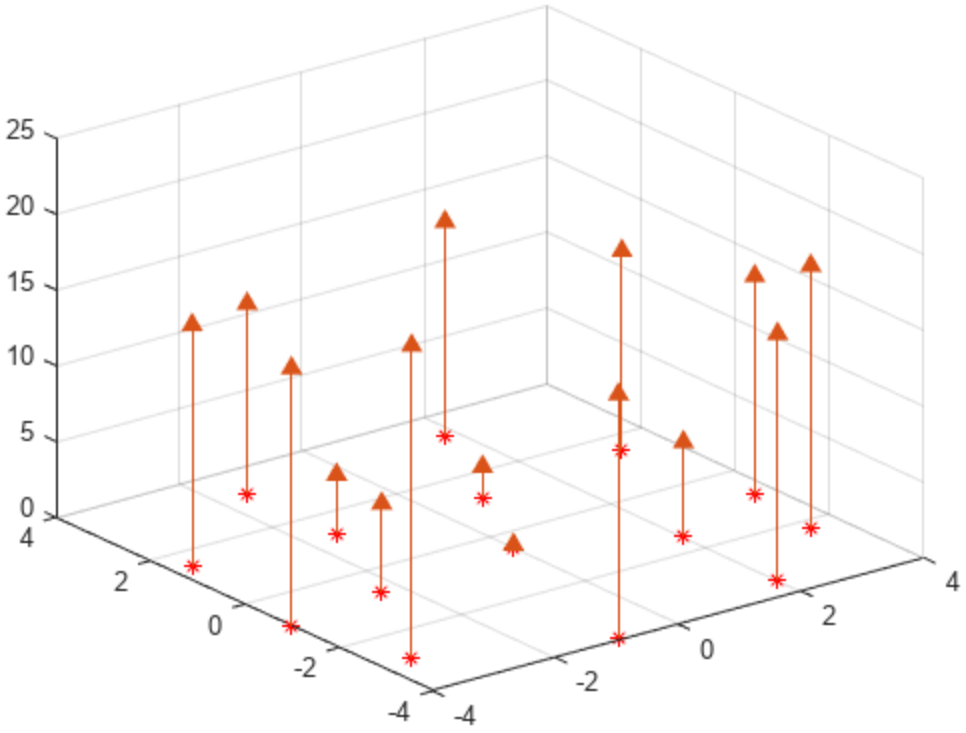

Figure 3.14 Lifting the vertices of the scattered data

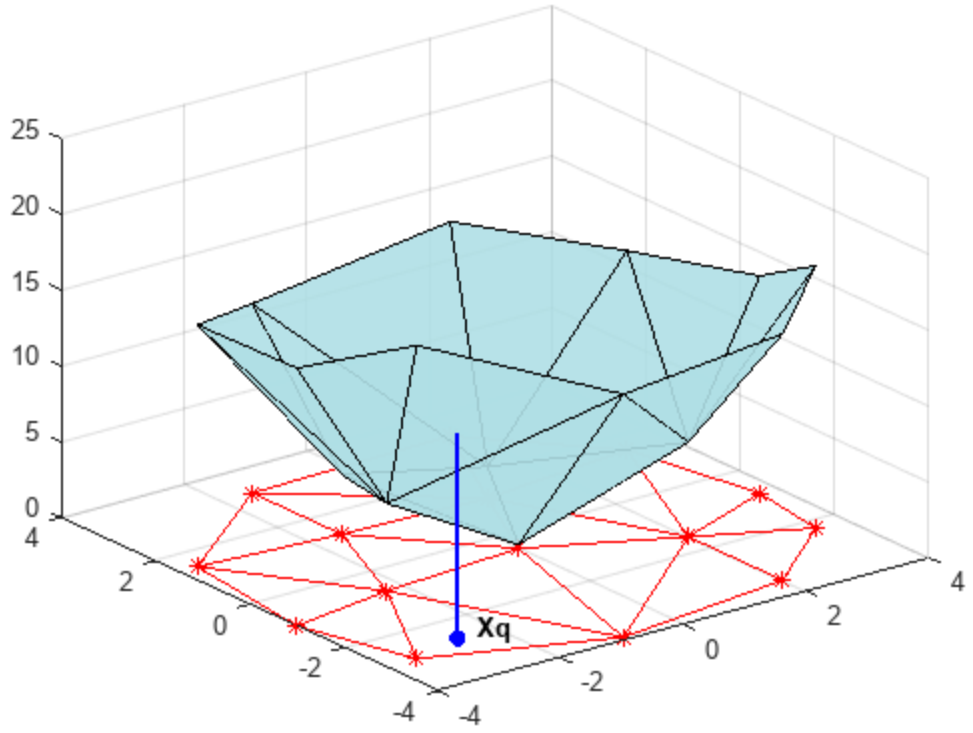

Figure 3.15 Delaunay triangulation to evaluate the interpolant at a query point Xq

The complexity of the Delaunay triangulation is not covered in this research. Although the interpolation process is broken into several steps, the scatteredinterpolant function helps to accomplish all these steps with just one function call. This method of interpolation provides more flexibility as it produces an interpolating function that can be queried efficiently especially in a case where the data does not have any structure between them. Also, the underlying triangulation is created once and can be reused for subsequent queries. ScatteredInterpolant also provides the advantage of being able to change the method of interpolation or the data points independently of the triangulation. Furthermore, data points can be incrementally added or even removed efficiently without triggering a complete re-computation as long as the data points been edited are relatively small compared to the sample points. In addition, scatteredInterpolant method of interpolation,

provides extrapolation functionality for approximating values of points that fall outside the convex hull.

The scatteredInterpolant function is described below.

$$F = scatteredInterpolant \tag{3.35}$$

$$F = scatteredInterpolant(x, y, v) \tag{3.36}$$

$$F = scatteredInterpolant(x, y, z, v) \tag{3.37}$$

$$F = scatteredInterpolant(P, v) \tag{3.38}$$

$$F = scatteredInterpolant(\_\_, Method) \tag{3.39}$$

$$F = scatteredInterpolant(\_\_, Method, ExtrapolationMethod) \tag{3.40}$$

3.211 $F = scatteredInterpolant$

This function creates an empty scattered data interpolant object.

3.212 $F = scatteredInterpolant(x, y, v)$

This function generates an interpolant that fits a surface of the form $F = (x, y)$. (x, y) are vectors that specify the (x, y) coordinates of the sample points and v contains the sample values for these points.

3.213 $F = scatteredInterpolant(x, y, z, v)$

This function generates a 3-D interpolant of the form $F = (x, y, z)$.

3.214 $F = scatteredInterpolant(P, v)$

This function details the coordinates of the sample points as an array. The row of P contains the (x, y, z) coordinates of the sample values.

3.215 $F = scatteredInterpolant(\_\_, Method)$

This function details an interpolation method: $'nearest',\ 'linear'(default),\ or\ 'natural'$

3.216 $F = scatteredInterpolant(\_\_, Method, ExtrapolationMethod)$

This function details both the interpolation and extrapolation methods. From the function above, the $Method\ and\ ExtrapolationMethod$ in the last two arguments can be any of the syntax below.

$Method$ can be: $'nearest',\ 'linear',\ or\ 'natural'$.

$ExtrapolationMethod$ can be: $'nearest',\ 'linear',\ or\ 'none'$.

An example of how the scatteredInterpolant is used is seen below.

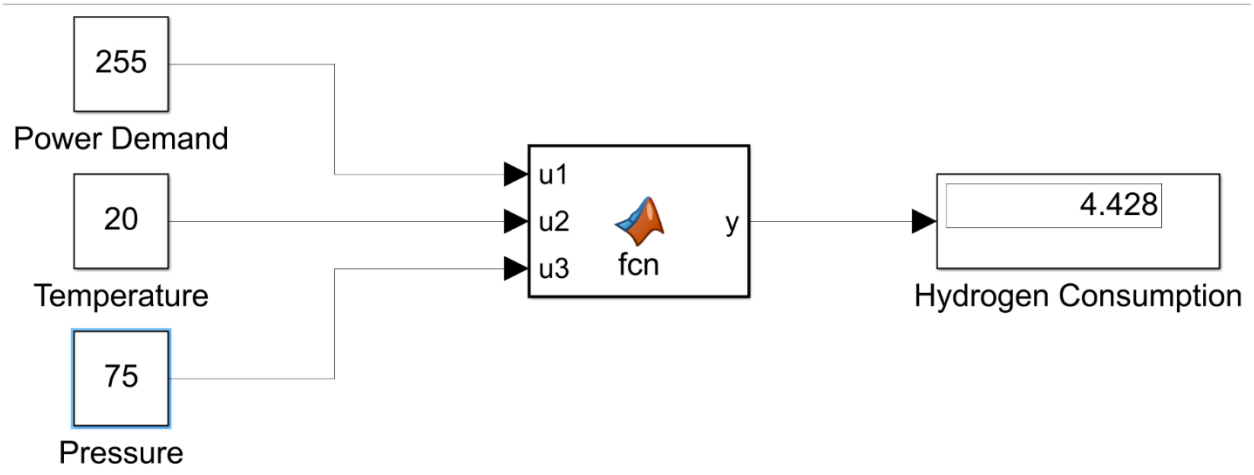

Figure 3.16 Using the scatteredInterpolant to calculate the hydrogen consumption

```
function y = fcn(u1,u2,u3)
% coder.extrinsic('scatteredInterpolant')  is required because function
% scatteredInterpolant is not available for code generation
coder.extrinsic('scatteredInterpolant')
%
y=1; % initializes variable type
PowerDemand = [250; 250; 144; 144; 93; 93; 22; 15];
Temperature = [-10; -28; -10; -43; -10; -33; -10; -28];
Pressure = [101.3000; 65.5000; 101.3000; 42.8000; 101.3000; 42.8000;101.3000; 65.5000];
HydrogenConsumption = [4.2400; 5.2000; 1.7500; 2.5400; 1.0000; 1.3400; 0.1700; 0.1400];
Fhydrogen = scatteredInterpolant(PowerDemand,Temperature,Pressure,HydrogenConsumption,'linear','linear');
%
y = Fhydrogen(u1,u2,u3);
```

Figure 3.17 ScattterInterpolant code written in the MATLAB function block

In figure 3.16, the scatteredInterpolant function in MATLAB is used to find the value of the hydrogen consumption when the power demand, temperature and pressure of the device is at 255KW, 20 Celsius and 75 KPa respectively. Figure 3.17 shows the code written in the MATLAB function block. Equation 3.35 is utilized here where PowerDemand, Temperature, and Pressure are the x, y, and z vectors that specify the coordinates of the sample points. HydrogenConsumption is the sample values v of these points, and the interpolation and extrapolation method are linear and linear respectively.

3.217 MATLAB/Simulink Function Block

Figure 3.18 MATLAB function block

This block helps one to write a MATLAB function for use in a Simulink model. Double clicking the MATLAB Function block opens the editor where the code can be written.

3.2171 Input

u – Input argument u

This is the first input argument of the function inside the MATLAB Function block. Renaming this function argument in the editor also renames the port correspondingly.

n – Input argument n

Adding n input in the editor, adds n input argument to the function in the MATLAB Function block correspondingly.

3.2172 Output

y – Output argument y

This is the first output argument of the function inside the MATLAB Function block. Renaming this function argument in the editor also renames the port correspondingly.

n – Input argument

Adding n input in the editor, adds n input argument to the function in the MATLAB Function block correspondingly.

3.22 The Interp1 Function Model

The interp1 function is a linear interpolation by default. This can be changed to other forms, but the principle behind the additional point generation is the same. Linear interpolation is a simple

method that is used to estimate the value of a particular function between two given values. Unlike the scattered data interpolation, these given values have a defined structure and a relationship between them. As seen in figure 3.19 the new datapoint is obtained by connecting the adjacent known values with a straight line.

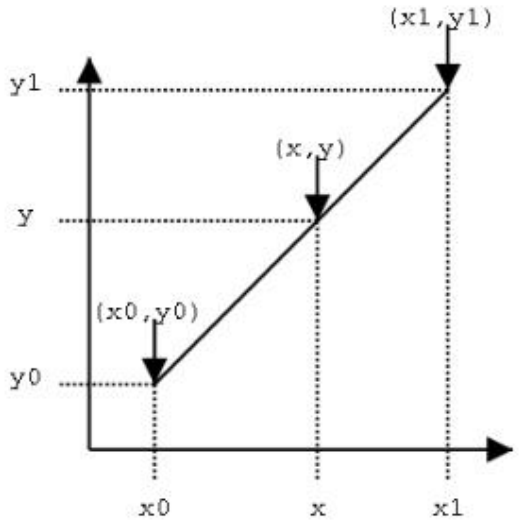

Figure 3.19 Linear interpolation

Linear interpolation $(y) = y_1 + (x - x_1)\frac{(y_2 - y_1)}{(x_2 - x_1)}$ (3.41)

Where:

x_1 and y_1 are the first coordinates.

x_2 and y_2 are the second coordinates

x is the point where the interpolation is to be performed and

y is the interpolated data point.

The interp1 function can be written in the different forms:

$vq = interp1(x, v, xq)$ (3.42)

$$vq = interp1(x, v, xq, method) \quad (3.43)$$

$$vq = interp1(x, v, xq, method\ extrapolation) \quad (3.44)$$

3.221 $vq = interp1(x, v, xq)$

Using the linear interpolation method, this function returns the interpolated values at specific selected points. Here, x is a vector that contains the sample points, while v is the corresponding values, v(x). xq is the vector that contains the coordinates of the selected points.

3.222 $vq = interp1(x, v, xq, method)$

The difference between equation 3.34 and 3.35 is that for equation two, an alternative interpolation method such as ‘nearest’, ‘spline’, or ‘cubic’ can be specified rather than using only the default method (linear)

3.223 $vq = interp1(x, v, xq, method, extrapolation)$

The addition of extrapolation here helps to evaluate points that lie outside of the domain of x. If the goal is to employ the method algorithm for extrapolation, then the term extrapolation in the function above is specified as ‘extrap’.

The interp1 function was utilized in this research to generate additional data points for the various parameters needed for the fuel cell powered aircraft.

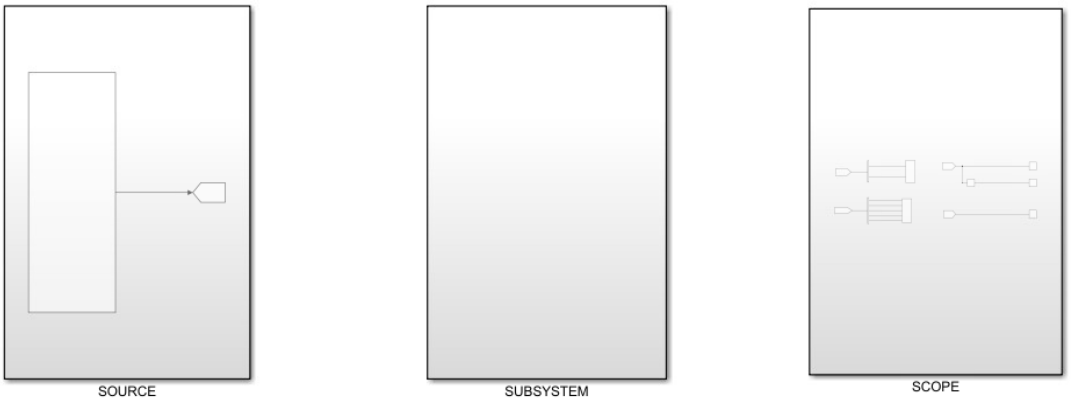

Figure 3.20 Fuel cell system

The interp1 function was used to derive several data points of a fuel cell system. The system as seen in figure 3.20 is made up of the source, the subsystem, and the scope.

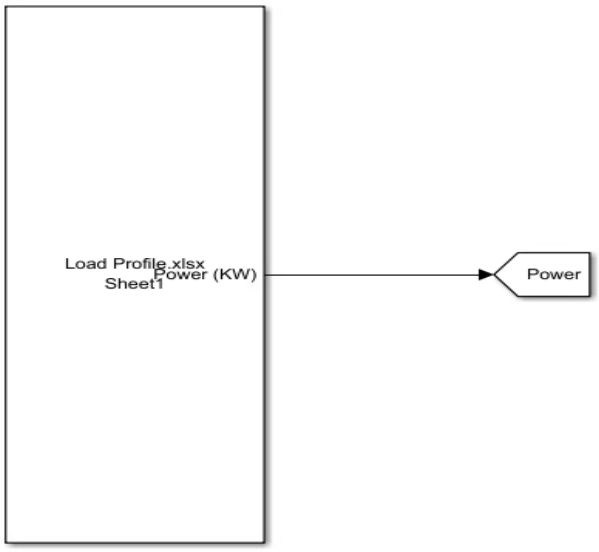

Figure 3.21 The source of the fuel cell system

The source contains the time of flight and power demand of an aircraft that uses a fuel cell system as its means of power. The power is in kilowatts and the time of flight captures the complete duration of flight and several intervals during the flight and the required power at these intervals.

Table 3.1 Load Profile

Time (s)	**Power (KW)**
0	0
1	415
30	415
30	232
60	232
60	141
590	141
590	120
610	120
610	100
1000	100
1000	170
1350	170
1350	350
1400	350
1400	65
2000	65
2000	400
2050	400
2050	200
2110	200
2110	120
2500	120
2500	130
2800	130
2800	110
3200	110
3200	140
3400	140
3400	300
3550	300
3550	65

3750	65
3750	400
3900	400
3900	200
3970	200
3970	110
4350	110
4350	115
4600	115
4600	108
5300	108
5300	130
5350	130
5350	300
5390	300
5390	0

The load profile which shows the power demand at each time during the flight duration of the aircraft can be seen in table 3.1. The time is in seconds while the power is in kilowatts.

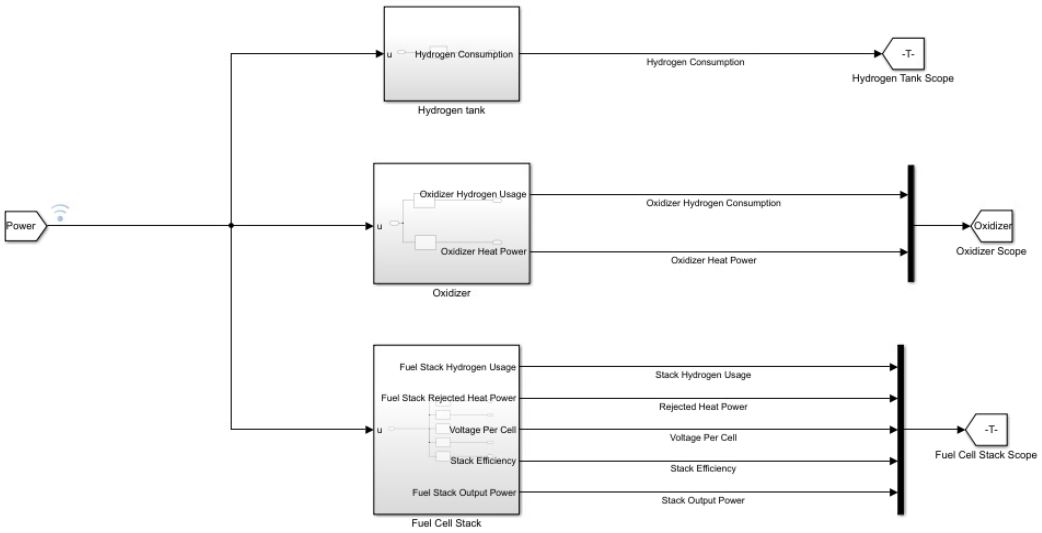

Figure 3.22 The subsystem of the fuel cell

The subsystem, Figure 3.22 shows several blocks highlighted in this model which are the hydrogen tank where the hydrogen fuel cell is stored, the oxidizer and the fuel cell stack.

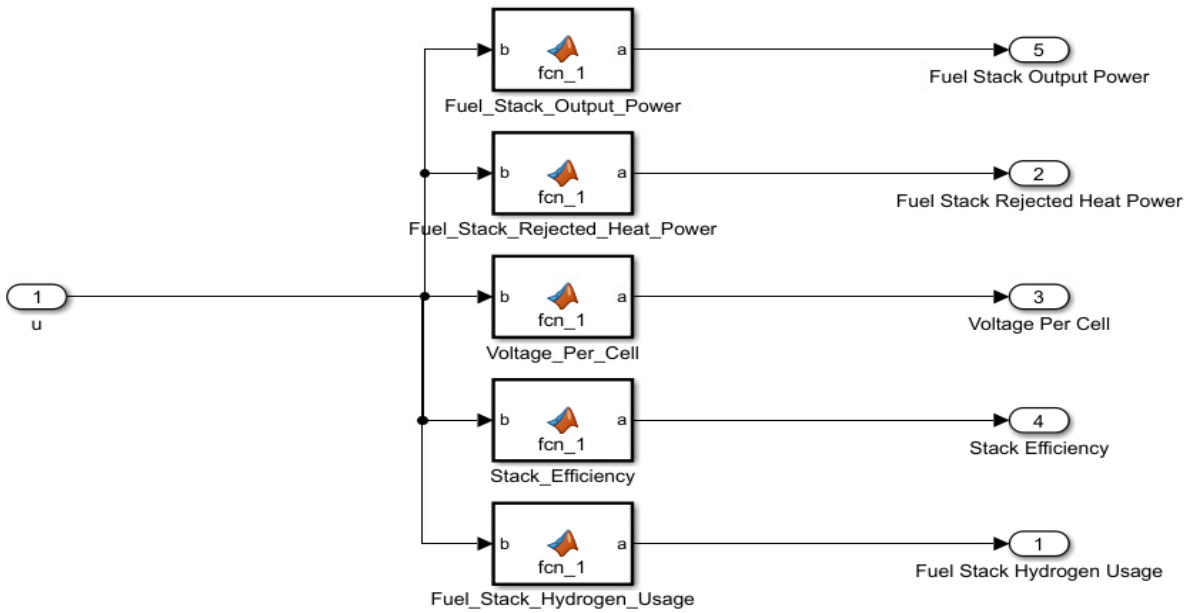

Figure 3.23 The fuel cell stack

A look into the set-up of one of the blocks, the fuel cell stack, shows some of the parameters listed. In figure 3.23, the following parameters are seen above, fuel stack out power, fuel stack rejected heat power, voltage per cell, stack efficiency and fuel stack hydrogen usage.

```
function a = fcn_1(b)
power=[100 250];
Fuel_Stack_Output_Power = [110 295];
a = interp1(power, Fuel_Stack_Output_Power, b, 'linear', 'extrap');
```

Figure 3.24 The fuel stack output power MATLAB function block

```
function a = fcn_1(b)
power=[110.2 250];
Fuel_Stack_Hydrogen_Usage = [1.9 5.8];
a = interp1(power, Fuel_Stack_Hydrogen_Usage, b, 'linear', 'extrap');
```

Figure 3.25 The fuel stack hydrogen usage MATLAB function block

```
function a = fcn_1(b)
power=[110.2 250];
StackEfficiency = [47.2 43];
a = interp1(power, StackEfficiency, b, 'linear', 'extrap');
```

Figure 3.26 The fuel stack efficiency MATLAB function block

Figure 3.24, 3.25, and 3.26 shows the code in fuel stack output power, fuel stack hydrogen usage, and fuel stack efficiency MATLAB function block. The code takes the form of the equation 3.44. As can be seen in the three figures, only two data points are provided. The use of the interp1 function helps to derive other data points needed.

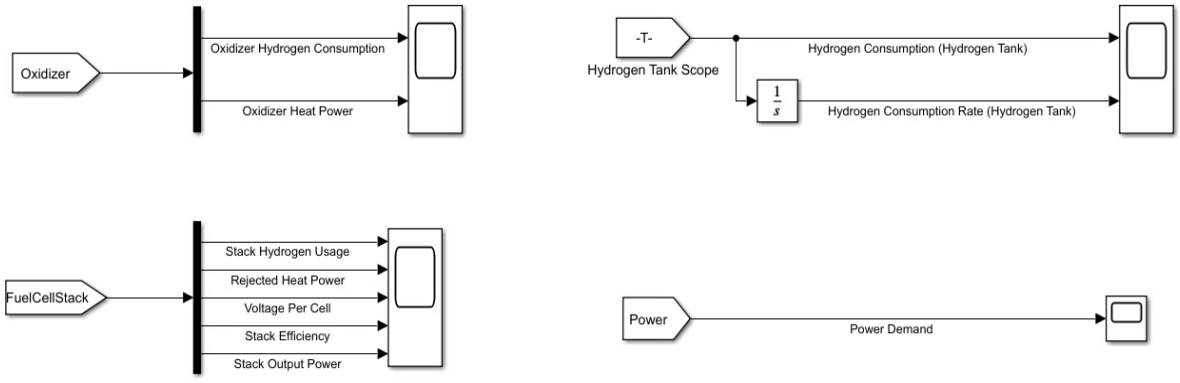

Figure 3.27 The scope of the fuel cell system

The scope in figure 3.27 shows the output waveform. The output waveforms are the waveform of the oxidizer, fuel cell stack, hydrogen tank and the power demand.

CHAPTER 4

RESULT AND DISCUSSION

4.1 Power Fuel Cell Model Results

The waveforms below show the behavior of the load which is a series resistor and inductor circuit. The initial increase of the fuel cell current from 0s to 5s is due to the 1s time constant of the RL load at the output of the Boost converter. As current begins to flow through the circuit, the current does not rise rapidly as determined by ohm's law due to the limiting factor created by the self-induced emf within the inductor as a result of the growth of the magnetic flux. At a certain point the voltage from the PEM fuel cell neutralizes the effect of the self-induced emf and the current flow becomes constant and the induced current and field reduces to zero.

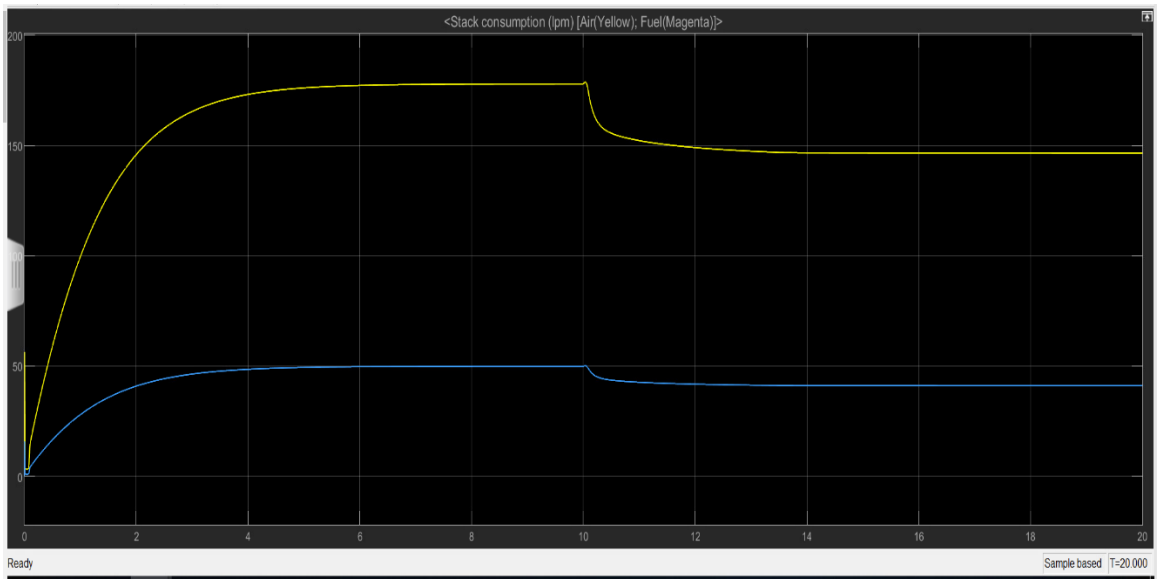

Figure 4.1. Stack consumption with the flow rate regulator bypassed

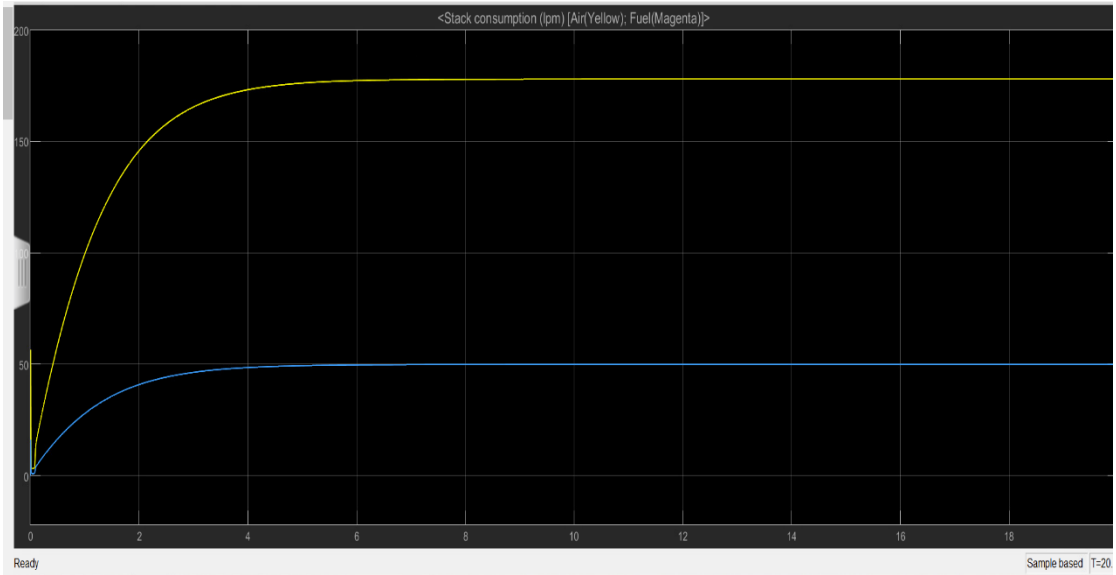

Figure 4.2 Stack consumption with the flow rate regulator not bypassed.

In figure 4.1, the yellow line shows the stack consumption of air while the magenta line represents the stack consumption of hydrogen. It can be seen that there is an increase in air and fuel consumption from the start to the 10 second mark. At this point, the stack consumption of air reaches a maximum value of 178.2 lpm and the stack consumption of fuel reaches a maximum value of 49.9 lpm. After this point, both values start decreasing until they reach a steady state at about 15 sec.

For figure 4.2, the regulator is not bypassed, and it can be seen that there is a steady increase from the start of the operation until it reaches steady at about 5 seconds.

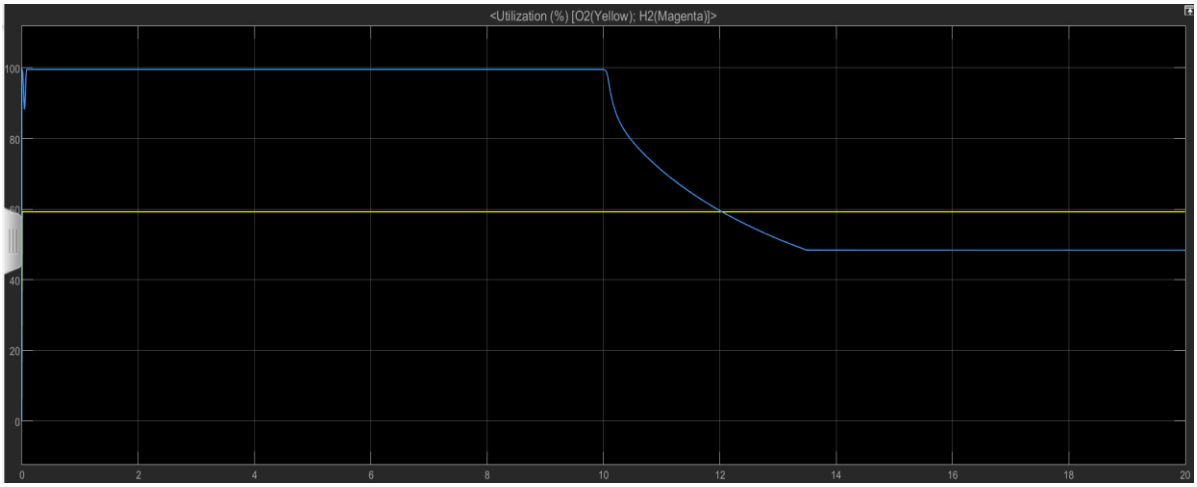

Figure 4.3. Stack utilization with the flow rate regulator bypassed

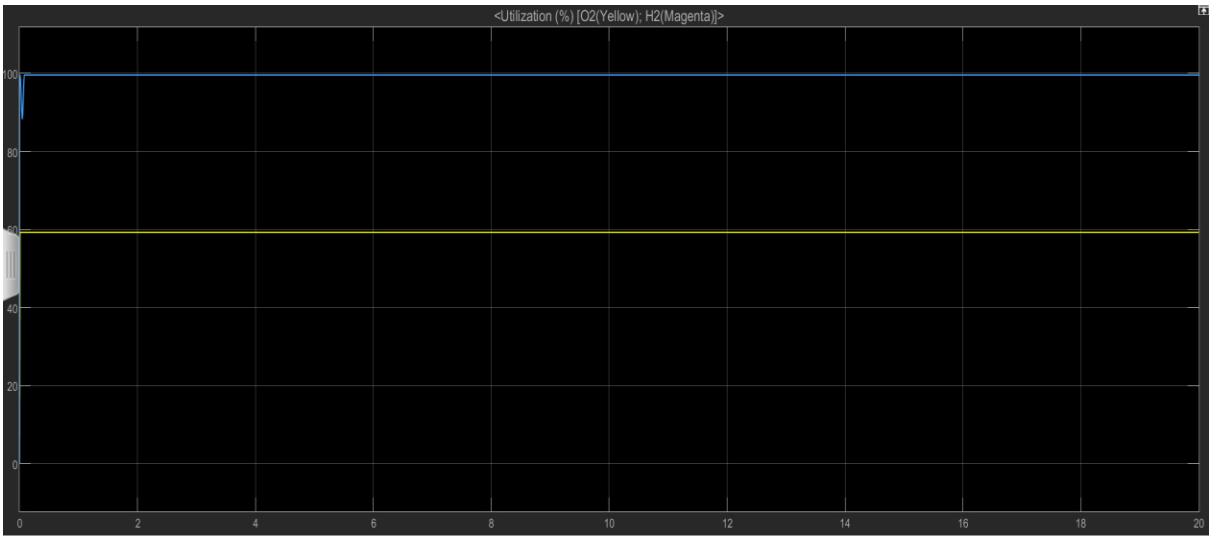

Figure 4.4 Stack consumption with the flow rate regulator not bypassed.

The utilization of the hydrogen and oxygen in the fuel stack is seen in figures 4.3 and 4.4. In figure 4.3, the flow rate regulator is not bypassed, and the utilization of hydrogen is maintained at approximately 100%. Figure 4.4 shows a drop in the utilization of hydrogen as the flow rate is bypassed. The reactant consumption in figure 4.1 and 4.2 shows the amount of the reactants that the stack consumes with time, figure 4.3 and 4.4 shows the percentage of reactants utilized in other to produce power.

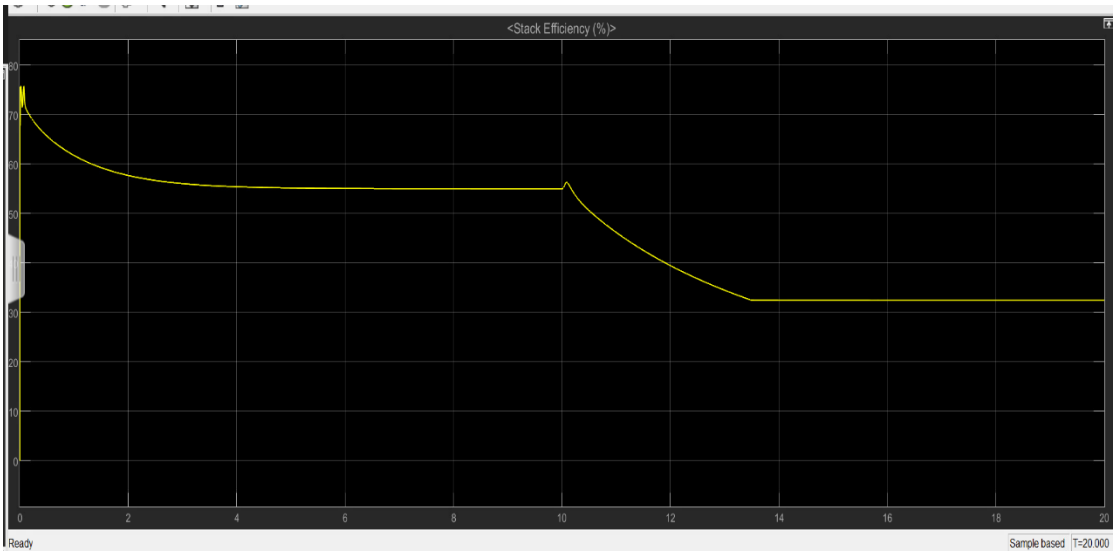

Figure 4.5 Stack efficiency with the flow rate regulator bypassed

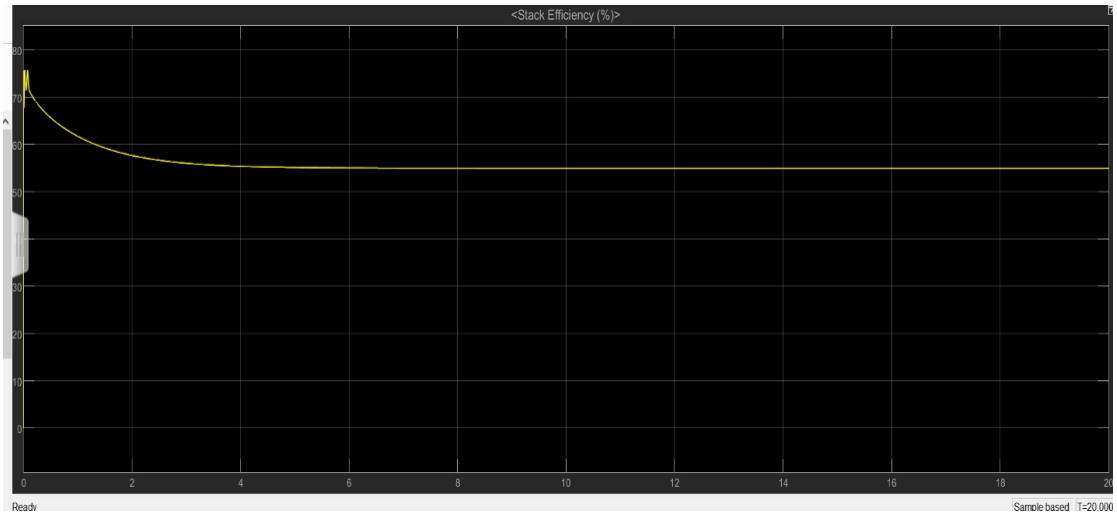

Figure 4.6 Stack efficiency with the flow rate regulator not bypassed.

The stack efficiency is seen in figures 4.5 and 4.6 respectively. Figure 4.5 shows the stack efficiency when the flow rate regulator is bypassed at 10 seconds. The efficiency of a fuel cell at any point in time is based on the voltage per cell and the utilization of the fuel as seen in equation 3.11. The drop in the utilization contributes to the transient experienced in the efficiency from 10s to 13s. Figure 4.6 shows the efficiency of the fuel cell when the flow rate regulator is not bypassed.

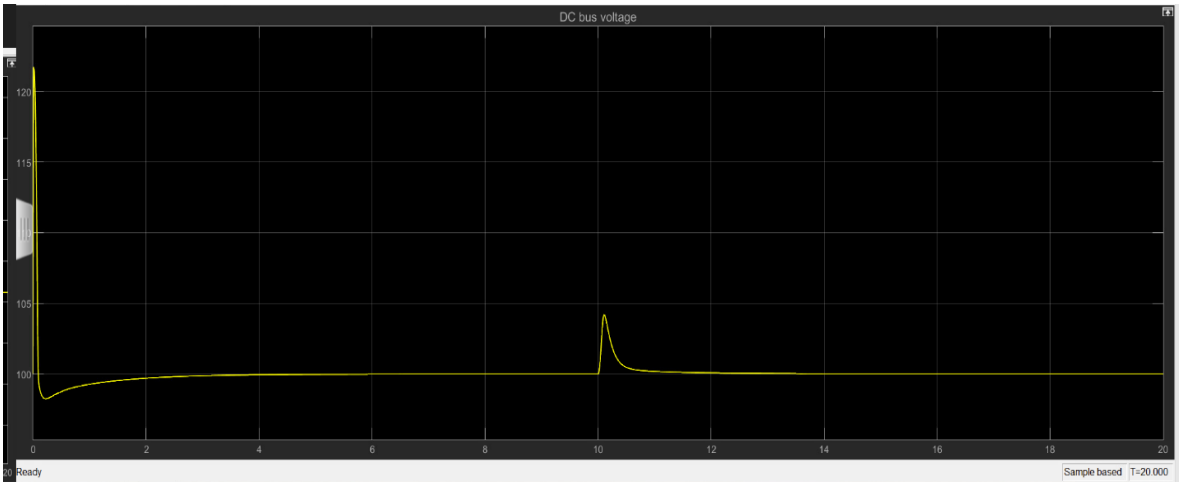

Figure 4.7 DC bus voltage with the flow rate regulator bypassed

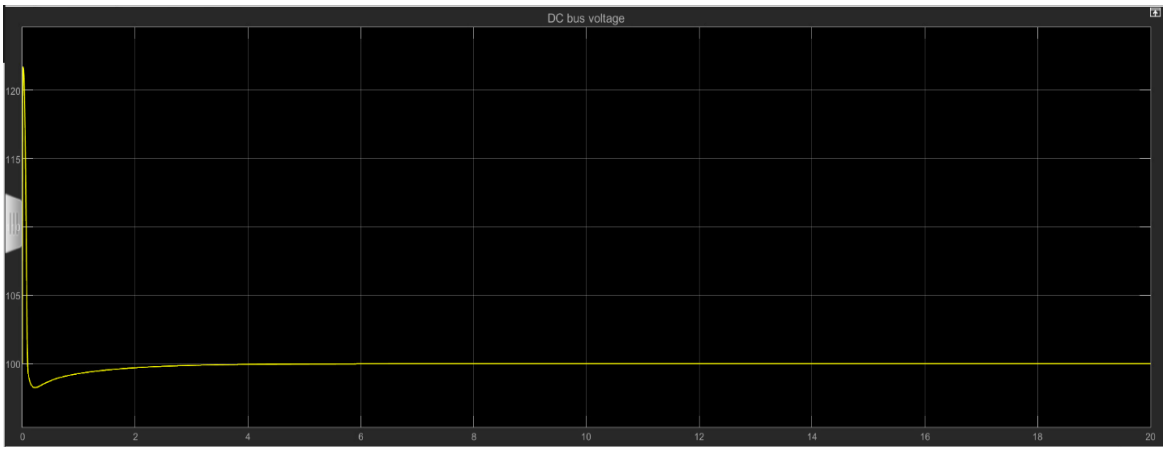

Figure 4.8 DC bus voltage with the flow rate regulator not bypassed.

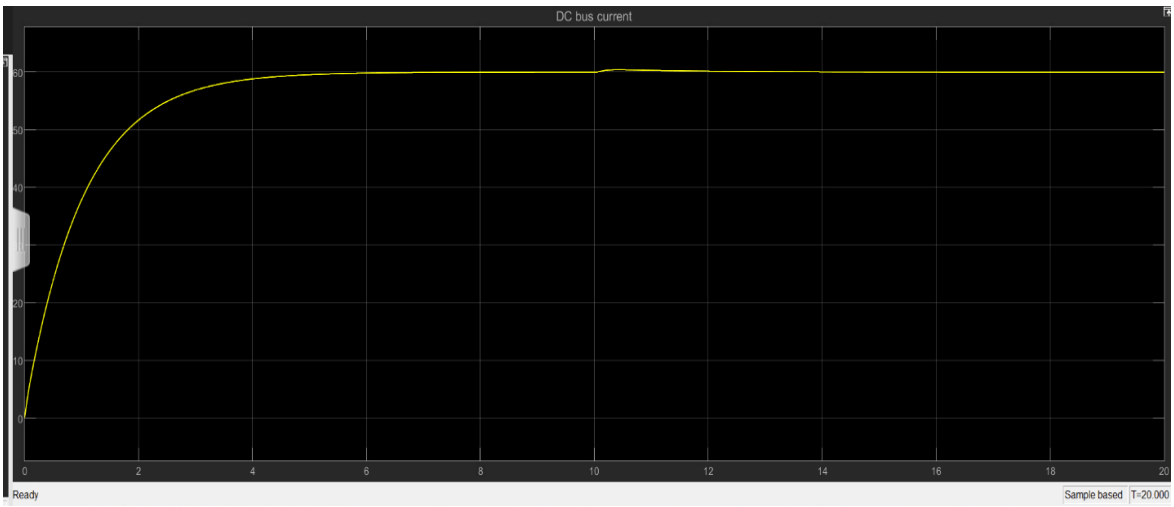

Figure 4.9 DC bus current with the flow rate regulator bypassed

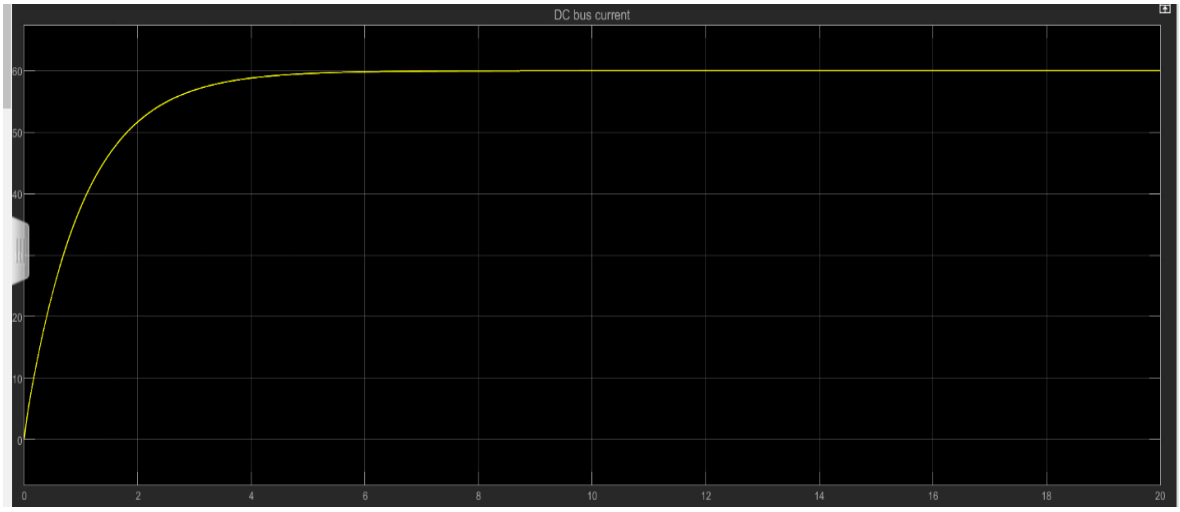

Figure 4.10 DC bus voltage with the flow rate regulator not bypassed.

In figures 4.7 and 4.9, the characteristics of the DC bus voltage and Dc bus current are analyzed respectively. There is an increase from the start of the operation until the regulator bypassed at time 10 sec. The value of the DC bus voltage at 10.1 sec is 104.1 V and the value of the DC bus current at 10.1 sec is 60.3 A. The waveform reaches a steady state in 15 seconds.

For Fig 4.8 and 4.10, the regulator is not bypassed, and it can be seen that there is a steady increase from the start of the operation until it reaches steady at about 5 sec.

4.2 Interp1 Function Model Results

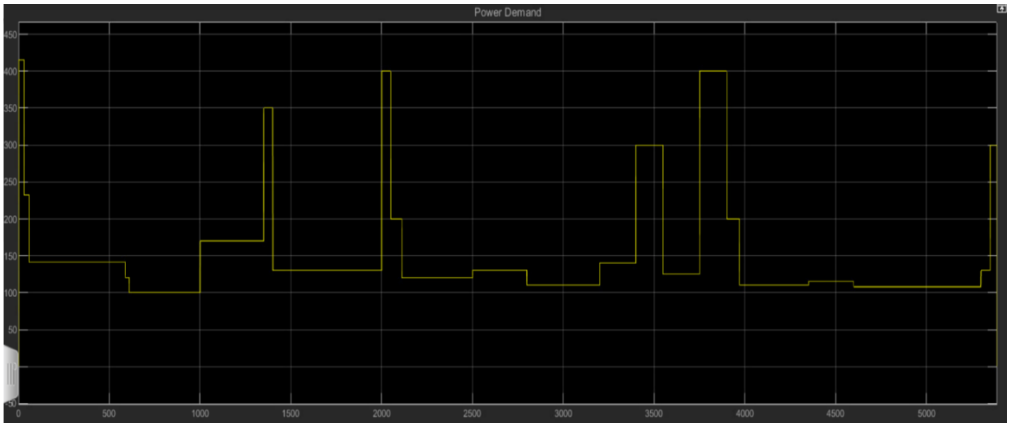

Figure 4.11 Power demand of the aircraft

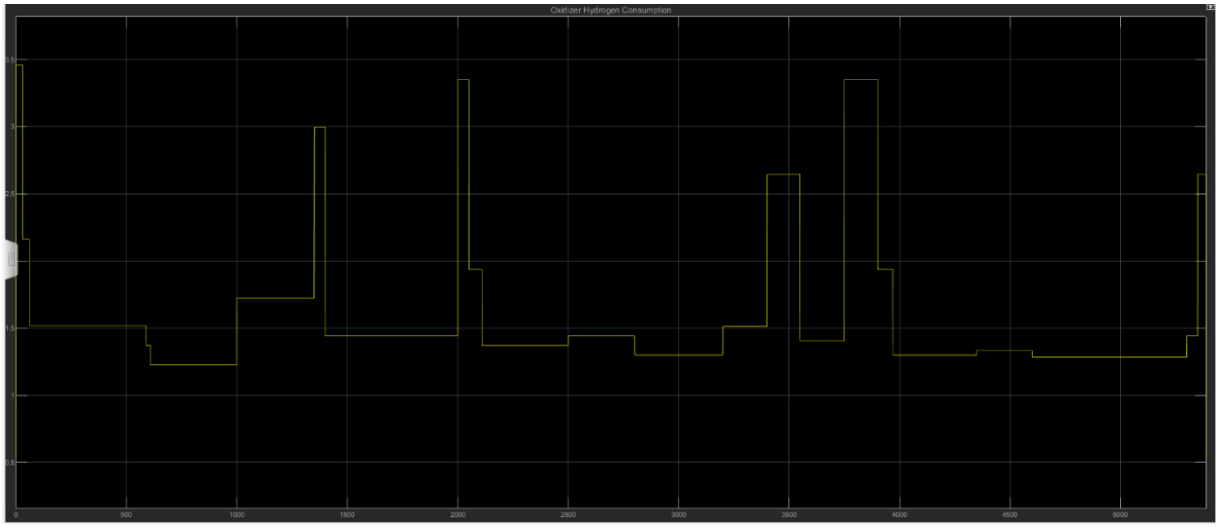

Figure 4.12 Oxidizer hydrogen consumption waveform

Table 4.1 Data points for the oxidizer hydrogen consumption

Time (s)	**Oxidizer Hydrogen Consumption**
0.01	0.5515
46	2.1627
231	1.5192
668	1.2293
1105	1.7243
1359	2.9971
2672	1.4414
4077	1.3
4906	1.2859
5390	0.5221

Figure 4.11 shows the power demand of fuel cell powered aircraft which is the complete flight profile of the aircraft. Figure 4.12 shows the oxidizer hydrogen consumption. The waveform was gotten by using the interp1 function to generate other data points in the experiment. Table 4.1 shows ten random points picked from the waveform in figure 4.12

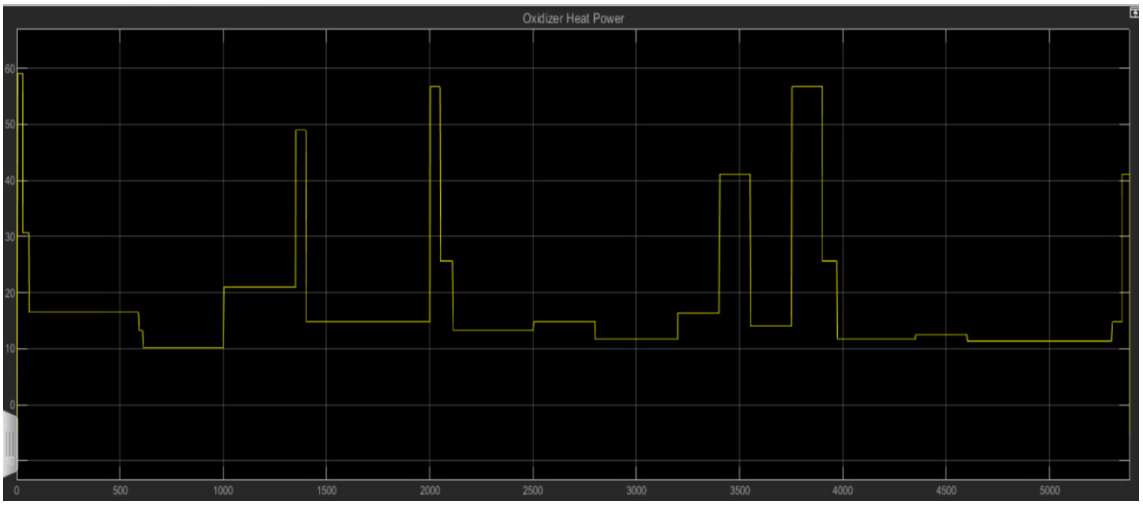

Figure 4.13 Oxidizer heat power waveform

Table 4.2 Data points for the oxidizer heat power

Time (s)	**Oxidizer Heat Power**
0.1	1.0192
46	30.6045
231	16.4719
668	10.1045
1105	20.9757
1359	48.93035
2672	14.7636
4077	11.6575
4906	11.3469
5389.9	41.1652

Using the interp1 function we are able to get more data points for the oxidizer heat power. The result is seen in the waveform in figure 4.13. This result aligns with the result gotten under real time scenario. Table 4.2 shows ten random points picked from the waveform in figure 4.13.

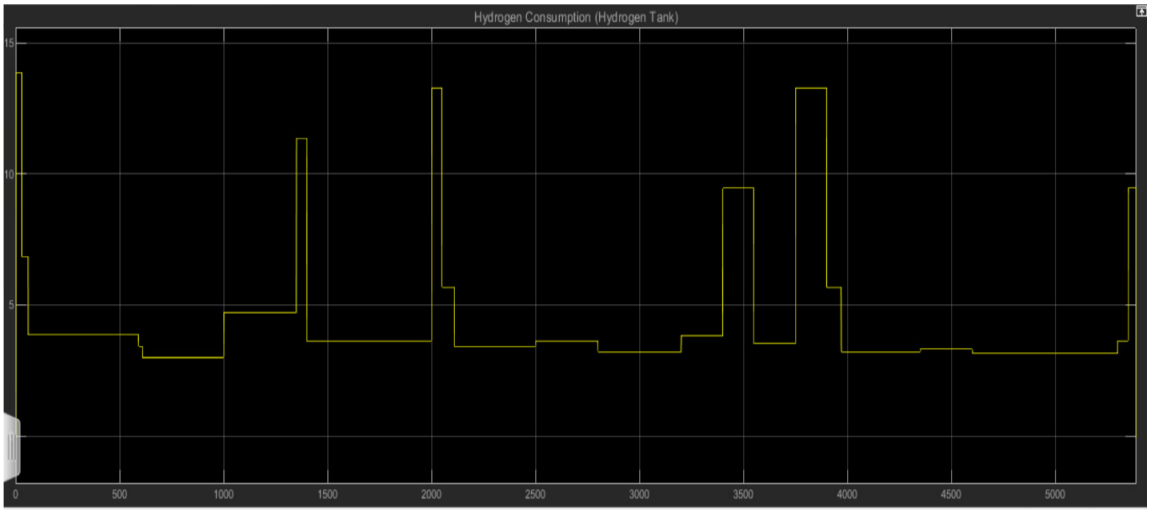

Figure 4.14 Hydrogen consumption from the hydrogen tank

Table 4.3 Data points for the hydrogen consumption (hydrogen tank)

Time (s)	**Hydrogen Consumption (Tank)**
0.1	1.19
46	6.8508
231	3.8609
668	10.1045
1105	4.7033
1359	11.3603
2672	3.6298
4077	3.2096
4906	3.1676
5389.9	9.4495

Using the interp1 function we are able to get more data points for the hydrogen consumption from the hydrogen tank. The result is seen in the waveform in figure 4.14. This result aligns with the result gotten under real time scenario. Table 4.3 shows ten random points picked from the waveform in figure 4.14

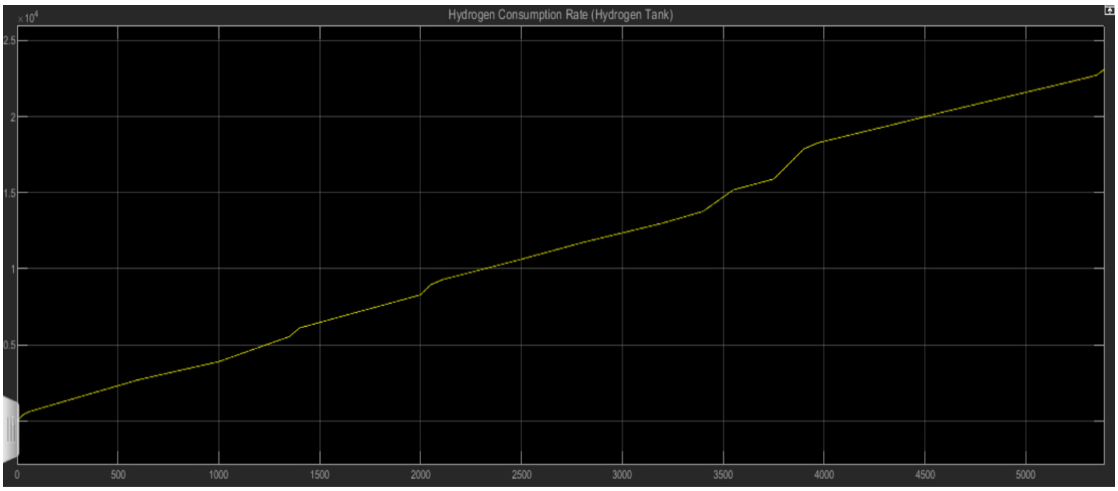

Fig 4.15 Hydrogen consumption rate from the hydrogen tank

Table 4.4 Data points for the hydrogen consumption rate (hydrogen tank)

Time (s)	**Hydrogen Consumption Rate (Hydrogen Tank) grams**
0.1	0.055
46	517.5053
231	1273.631
668	2901.777
1105	4389.827
1359	5644.386
2672	11250.6
4077	18621.34
4906	21295.5
5389.9	23102.05

Using the interp1 function we are able to get more data points for the hydrogen consumption rate for the hydrogen usage in tank. This is done by integrating the values from figure 4.4. This gives us a good estimate of the amount of hydrogen required for this flight. The result is seen in the waveform in figure 4.15. This result aligns with the result gotten under real time scenario. Table 4.4 shows ten random points picked from the waveform in figure 4.15

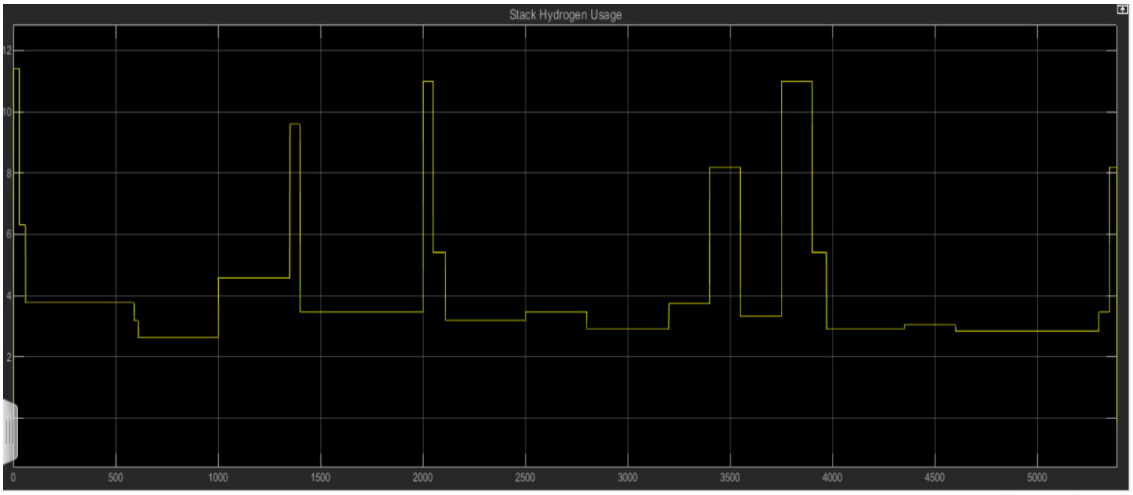

Figure 4.16 Stack hydrogen consumption

Table 4.5 Data points for the stack hydrogen consumption

Time (s)	Stack Hydrogen Consumption (g/s)
0.1	0.9835
46	6.2979
231	3.7592
668	2.6155
1105	4.5682
1359	9.5897
2672	3.4524
4077	2.8944
4906	2.8386
5389.9	8.1949

The stack hydrogen consumption is the hydrogen used up by the fuel cell stack during the course of the flight. Using the interp1 function we are able to get more data points as opposed to the few data points provided initially for the hydrogen consumption in the stack. The result can be seen in the waveform in figure 4.16. This result aligns with the result gotten under real time scenario. Table 4.5 shows ten random points picked from the waveform in figure 4.16.

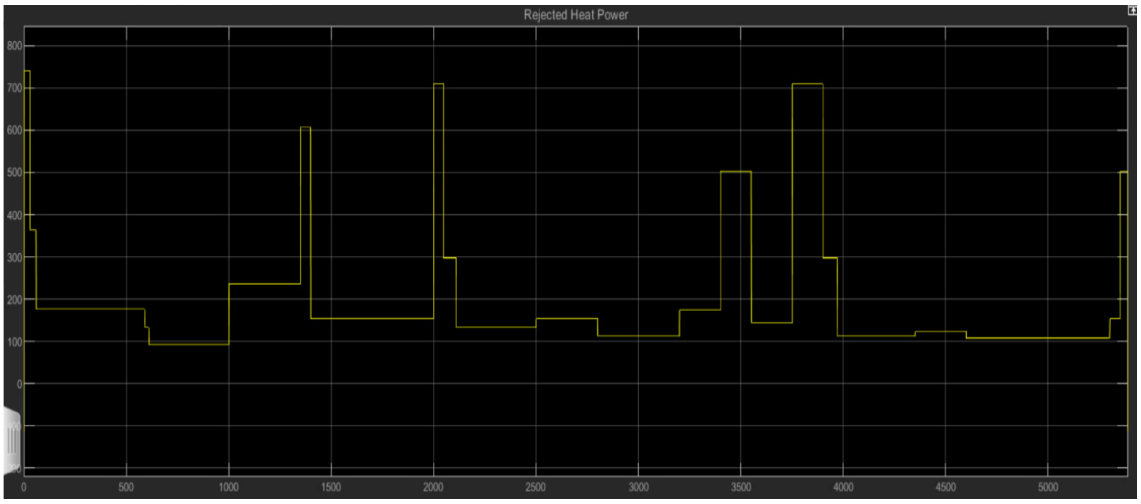

Figure 4.17 Stack rejected heat power

Table 4.6 Data points for the stack rejected heat power

Time (s)	Stack Rejected Heat Power (KW)
0.2	56.5993
46	363.4329
231	176.0379
668	91.6071
1105	235.7571
1359	606.4286
2672	153.3857
4077	112.2
4906	108.0814
5389.9	503.4643

Using the interp1 function we are able to get more data points for the rejected heat power from the fuel stack. The result is seen in the waveform in figure 4.17. This result aligns with the result gotten under real time scenario. Table 4.6 shows ten random points picked from the waveform in figure 4.17

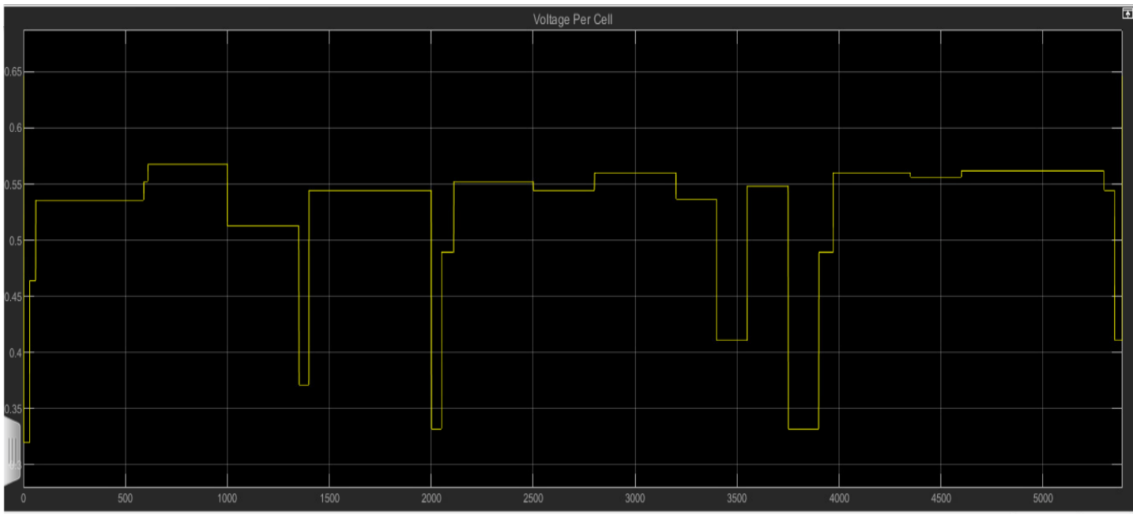

Figure 4.18 Voltage per cell

Table 4.7 Data points for voltage per cell

Time (s)	**Voltage Per Cell (V)**
0.1	0.6141
46	0.4641
231	0.5358
668	0.568
1105	0.513
1359	0.3713
2672	0.5444
4077	0.5602
4906	0.5617
5389.9	0.4107

The voltage per cell is the voltage of each cell in the fuel cell stack. Using the interp1 function we are able to get more data points as opposed to the few data points provided initially for the voltage per cell in the stack during the course of the flight. The result can be seen in the waveform in figure 4.18. This result aligns with the result gotten under real time scenario. Table 4.7 shows ten random points picked from the waveform in figure 4.18.

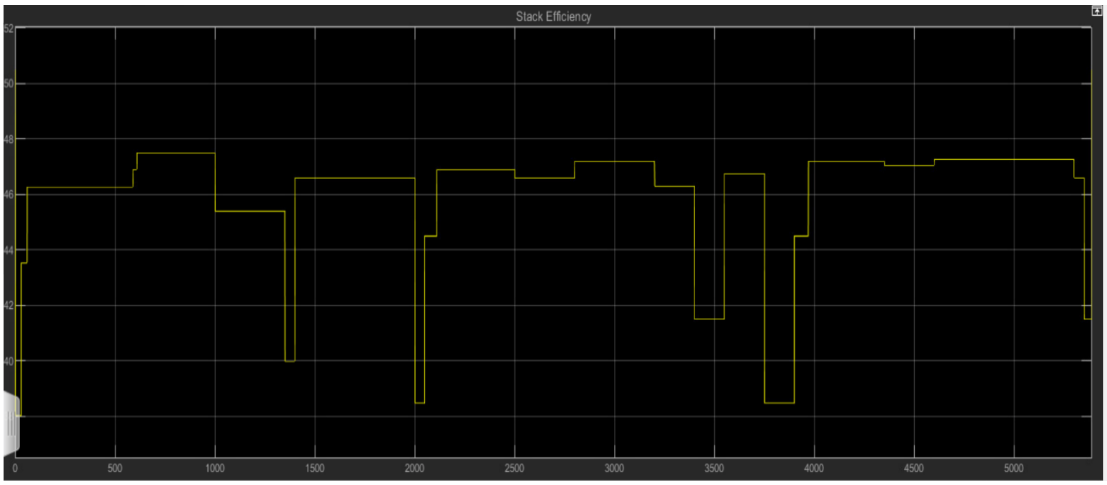

Figure 4.19 Stack efficiency

Table 4.8 Data points for stack efficiency

Time (s)	**Stack Efficiency (%)**
0.1	49.5133
46	43.5408
231	46.2747
668	47.5064
1105	45.4034
1359	39.9957
2672	46.6052
4077	47.206
4906	47.2661
5389.9	41.4989

Using the interp1 function we are able to get more data points for the efficiency of the fuel stack. The result is seen in the waveform in figure 4.19. This result aligns with the result gotten under real time scenario. Table 4.8 shows ten random points picked from the waveform in figure 4.19

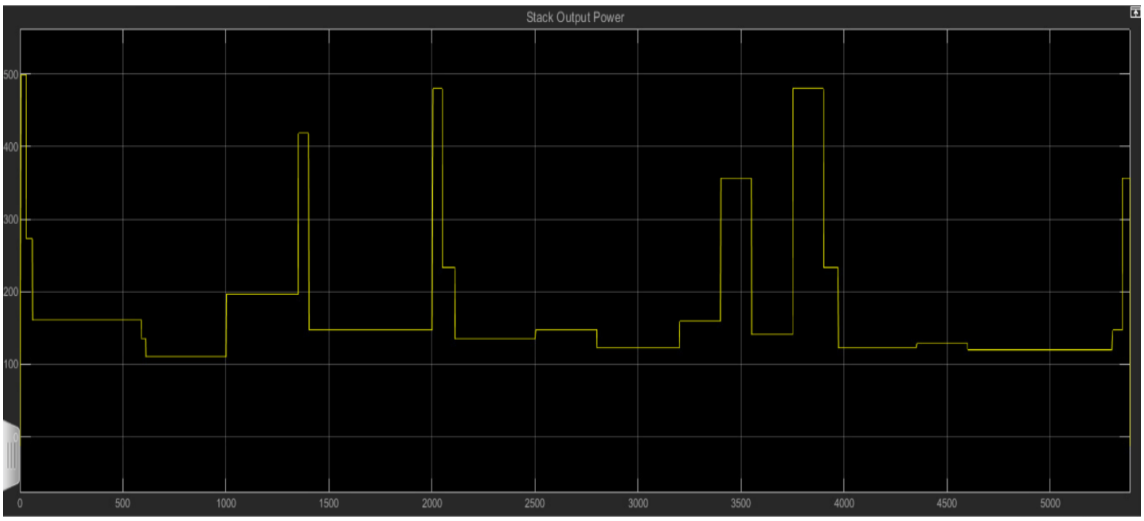

Figure 4.20 Stack output power

Table 4.9 Data points for stack output power

Time (s)	Stack Output Power (KW)
0.1	37.85
46	272.8
231	160.5667
668	110
1105	196.3333
1359	418.3333
2672	147
4077	122.3333
4906	119.8667
5389.9	356.6667

The stack output power is the output power produced by the fuel cell stack. Using the interp1 function we are able to generate more data points as opposed to the few data points provided initially for the output power from the fuel stack during the course of the flight. The result can be seen in the waveform in figure 4.20. This result aligns with the result gotten under real time scenario. Table 4.9 shows ten random points picked from the waveform in figure 4.20.

CHAPTER 5

CONCLUSION

This work analyzed the operation of a proton exchange membrane fuel cell. A detailed analysis of the important chemical reactions that occur in the fuel cell in order to generate electric energy was documented. The power fuel cell model in MATLAB/Simulink was used in the first part of this study and the results were carefully discussed. The waveform which includes the stack consumption, stack utilization, stack efficiency, dc bus current and bus voltage were analyzed when the flow rate regulator was bypassed after 10s and when it was not bypassed. The results, which are consistent with the detailed analysis of the chemical reaction discussed in the methodology showed a well-regulated voltage and current at the bus due to the applied DC/DC converter. For the set up that was not bypassed, the initial rise was due to the RL element which has a time constant of 1 sec, after this it maintained a steady state. When the set up was bypassed after 10 sec, the rate of fuel increased thereby reducing the hydrogen utilization, fuel current, stack efficiency and stack consumption. The voltage and current were properly regulated due to the application of the DC/DC converter. The result gotten from the simulation of the power fuel cell model is consistent with the chemical equations outlined in the methodology.

The second part of this research which is a behavioral model of the fuel cell involves the use of the scatteredInterpolant and interp1 function models. The result from these models showed how additional data points for the parameters needed for the research on fuel cells can be generated. These models were employed in the research conducted on fuel cell powered aircraft

and the result was similar to the mathematically generated data points in the laboratory. This proves to be an important model that can be used in further mathematical and computational studies.

REFERENCES

[1] Shimpalee S., Lilavivat, V., Van Zee, J.W, McCrabb, H, and Lozano-Morales, A. (2011). Understanding the effect of channel tolerances on performance of PEMFCs, Int. J. Hydrogen Energy 36:12512–12523.

[2] Mahjoubi, C, J. Olivier, J, S. Skander-mustapha, S, M. Machmoum, M, I. and Slama-belkhodja, I, (2018), An improved thermal control of open cathode proton exchange membrane fuel cell, Int. J. Hydrogen Energy 44: 11332–11345.

[3] Zhao, J. Jian,Q. Luo, L. Huang, B. Cao, S. and Huang, Z. (2018), Dynamic behavior study on voltage and temperature of proton exchange membrane fuel cells, Appl. Therm. Eng. 145: 343–351.

[4] Surtharssan, T, Montalvao, D, Chen, Y.K, Wang, W.C, Pisac, C, and Elemara, H. (2017). A review on prognostics and health monitoring of proton exchange membrane fuel cell, Renew. Sustain. Energy Rev. 75: 440–450.

[5] Qi, J. Zhai, Y. and St-Pierre, J. (2019). Effect of contaminant mixtures in air on proton exchange membrane fuel cell performance, J. Power Sources 413: 86–97.

[6] Elakkiya, S. Arthanareeswaran, G. Venkatesh, K. Kweon, J.(2018). Enhancement of fuel cell properties in polyethersulfone and sulfonated poly (ether ether ketone) membranes using metal oxide nanoparticles for proton exchange membrane fuel cell, Int. J. Hydrogen Energy 43: 21750–21759. ScienceDirect

[7] Kraytberg, Alexander, Yair Ein-Eli, (2014). Review of Advanced Materials for Proton Exchange Membrane Fuel Cells, Energy fuel. 28

[8] Shao, H. Qiu, D. Peng, L. Yi,P. and Lai, X (2019). In-situ measurement of temperature and humidity distribution in gas channels for commercial-size proton exchange membrane fuel cells, J. Power Sources 412: 717–724.

[9] Vijay Babu, A.R. Manoj Kumar, P. and Srinivasa Rao, G. (2018). Parametric study of the proton exchange membrane fuel cell for investigation of enhanced performance used in fuel cell vehicles, Alexandria Eng. J. 57 3953–3958.

[10] Lim, B.H. Majlan, E.H. Daud,W.R. Rosli, W M.I and Husaini, T. (2019. Three-dimensional study of stack on the performance of the proton exchange membrane fuel cell, Energy 169: 338–343.

[11] Barbir, F. (2013). PEM Fuel cells, second ed

[12] Pei, P. Jia, X. Xu, H. Li, P. Wu, Z. Li, Y. Ren, P. Chen, D. and HuangS., The recovery mechanism of proton exchange membrane fuel cell in micro- current operation, Appl. Energy 226 (2018) 1–9.

[13] Dekel, D.R. (2018), Review of cell performance in anion exchange membrane fuel cells, J. Power Sources 375 158–169

[14] Mehta, V. and Cooper, J.S. (2003) Review and analysis of PEM fuel cell design and manufacturing, J. Power Sources 114 32–53.

[15] Kec ̧eci M et al., Reducing the fuel consumption and emissions with the use of an external fuel cell hybrid power unit for electric taxiing at airports, International Journal of Hydrogen Energy, https://doi.org/10.1016/j.ijhydene.2022.04.27

[16] Guida, D., & Minutillo, M. (2017). Design methodology for a PEM fuel cell power system in a more electrical aircraft. Applied energy, 192, 446-456.

[17] Pratt, J. W., Klebanoff, L. E., Munoz-Ramos, K., Akhil, A. A., Curgus, D. B., & Schenkman, B. L. (2013). Proton exchange membrane fuel cells for electrical power generation on-board commercial airplanes. Applied energy, 101, 776-796.

[18] Campanari, S., Manzolini, G., Beretti, A., & Wollrab, U. (2008). Performance assessment of turbocharged PEM fuel cell systems for civil aircraft onboard power production. Journal of engineering for gas turbines and power, 130(2).

[19] Lüdders, H.P., Strummel, H. & Thielecke, F. Model-based development of multifunctional fuel cell systems for More-Electric-Aircraft. CEAS Aeronaut J 4, 151–174 (2013).

[20] Kadyk, T., Winnefeld, C., Hanke-Rauschenbach, R., & Krewer, U. (2018). Analysis and design of fuel cell systems for aviation. Energies, 11(2), 375.

[21] Schröter, J., Graf, T., Frank, D., Bauer, C., Kallo, J., & Willich, C. (2021). Influence of pressure losses on compressor performance in a pressurized fuel cell air supply system for airplane applications. International Journal of Hydrogen Energy, 46(40), 21151-21159.

[22] Werner, C., Busemeyer, L., & Kallo, J. (2015). The impact of operating parameters and system architecture on the water management of a multifunctional PEMFC system. International Journal of Hydrogen Energy, 40(35), 11595-11603.

[23] Futter, G.A., Gazdzicki P., Friedrich K.A., Latz A., Jahnke T. (2018). Physical modeling of polymer-electrolyte membrane fuel cells: understanding water management and impedance spectra. J Power Sources, 391, pp. 148-161.

[24] Salva J.A., Iranzo A., Rosa F., Tapia E., Lopez E., Isorna F. (2016). Optimization of PEM fuel cell operating conditions: obtaining the maximum performance polarization curve. Int J Hydrogen Energy, 41 (43), pp. 19713-19723

[25] Goshtasbi, A., Pence, B. L., Chen, J., DeBolt, M. A., Wang, C., Waldecker, J. R., ... & Ersal, T. (2020). A mathematical model toward real-time monitoring of automotive PEM fuel cells. Journal of The Electrochemical Society, 167(2), 024518.

[26] Kim, D. K., Seo, J. H., Kim, S., Lee, M. K., Nam, K. Y., Song, H. H., & Kim, M. S. (2014). Efficiency improvement of a PEMFC system by applying a turbocharger. International journal of hydrogen energy, 39(35), 20139-20150.

[27] Kim, D. K., Min, H. E., Kong, I. M., Lee, M. K., Lee, C. H., Kim, M. S., & Song, H. H. (2016). Parametric study on interaction of blower and back pressure control valve for a 80-kW class PEM fuel cell vehicle. International Journal of Hydrogen Energy, 41(39), 17595-17615.

[28] Chen, H., Liu, B., Liu, R., Weng, Q., Zhang, T., & Pei, P. (2020). Optimal interval of air stoichiometry under different operating parameters and electrical load conditions of proton exchange membrane fuel cell. Energy Conversion and Management, 205, 112398.

[29] Qin, Y., Du, Q., Fan, M., Chang, Y., & Yin, Y. (2017). Study on the operating pressure effect on the performance of a proton exchange membrane fuel cell power system. Energy Conversion and Management, 142, 357-365.

[30] Hoeflinger, J., & Hofmann, P. (2020). Air mass flow and pressure optimization of a PEM fuel cell range extender system. International Journal of Hydrogen Energy, 45(53), 29246-29258

[31] J. Chen and Q. Song, "A Decentralized Dynamic Load Power Allocation Strategy for Fuel Cell/Supercapacitor-Based APU of Large More Electric Vehicles," in IEEE Transactions on Industrial Electronics, vol. 66, no. 2, pp. 865-875, Feb. 2019, doi: 10.1109/TIE.2018.2833031.

[32] Siangsanoh, A., Bahrami, M., Kaewmanee, W., Gavagsaz-ghoachani, R., Phattanasak, M., Martin, J. P., … Didierjean, S. (2020). *Series hybrid fuel cell/supercapacitor power source. Mathematics and Computers in Simulation.* doi: 10.1016/j.matcom.2020.02.001

[33] Pessot, A., Turpin, C., Jaafar, A., Soyez, E., Rallières, O., Gager, G., & d'Arbigny, J. (2019). Contribution to the modelling of a low temperature PEM fuel cell in aeronautical conditions by design of experiments. *Mathematics and Computers in Simulation, 158,* 179-198.

[34] Horde T., Achard P., metkemeijer R. (2012). PEMFC application for aviation: Experimental and nuerical study of sensitivity to altitude. Int. J. Hydrogen Energy, 37, pp. 10818-10829.

[35] Pratt J.W., Brouwer J., Samuelsen G.S. (2007). Performance of proton exchange membrane fuel cell at high-altitude conditions. J. Propul. Power, 23 (3).

[36] Kallo J., Renouard-Vallet G., Saballus M., Schmithals G., Schirmer J., Friedrich K.A. (2010). Fuel cell system development and testing for aircraft applications. 18th World Hydrogen Energy Conference, Proceedings, Essen, Germany, pp. 435-444.

[37] Werner, C., Preiß, G., Gores, F., Griebenow, M., & Heitmann, S. (2016). A comparison of low-pressure and supercharged operation of polymer electrolyte membrane fuel cell systems for aircraft applications. Progress in Aerospace Sciences, *85*, 51-64.

[38] Zhao, D., Xia, L., Dang, H., Wu, Z., & Li, H. (2022). Design and control of air supply system for PEMFC UAV based on dynamic decoupling strategy. Energy Conversion and Management, *253*, 115159.

[39] l-Hamed, K. H. M., & Dincer, I. (2020). Development and optimization of a novel solid oxide fuel cell-engine powering system for cleaner locomotives. Applied Thermal Engineering, 116150. doi:10.1016/j.applthermaleng.2020.116150

[40] Schröder, M., Becker, F., Kallo, J., & Gentner, C. (2021). Optimal operating conditions of PEM fuel cells in commercial aircraft. International Journal of Hydrogen Energy, 46(66), 33218–33240. doi:10.1016/j.ijhydene.2021.07.099

[41] Weigl, J. D., Henz, M., & Saidi, H. (2015). Converted battery-powered electric motorcycle and hydrogen fuel cell-powered electric motorcycle in South East Asia: Development and performance test. Proceedings of the Joint International Conference on Electric Vehicular Technology and Industrial, Mechanical, Electrical and Chemical Engineering (ICEVT & IMECE), IEEE. (pp. 1-4).

[42] Weigl, J. D., Henz, M., & Saidi, H. (2011). Development of hydrogen fuel cell motorcycle in South Asia. ECS Trans., 30 (1), p. 289.

[43] Chao, D. C. H., Van Duijsen, P. J., Hwang, J. J., & Liao, C. W. (2009). Modeling of a Taiwan fuel cell powered scooter. In 2009 International Conference on Power Electronics and Drive Systems (PEDS), IEEE, (pp. 913-919).

[44] Dicks L.A., Rand D.A.J. (2018) Fuel cell systems Explained, vol. 3, J. Wiley, Chichester, UK, pp. 207-225.

[45] MathWorks

www.mathwork.com